ISSN 1818-2712
J Nucl Med Tech
核 醫 技 學 誌

核醫技術學雜誌

Journal of Nuclear Medicine Technology

Journal of Nuclear Medicine Technology
核醫技術學雜誌

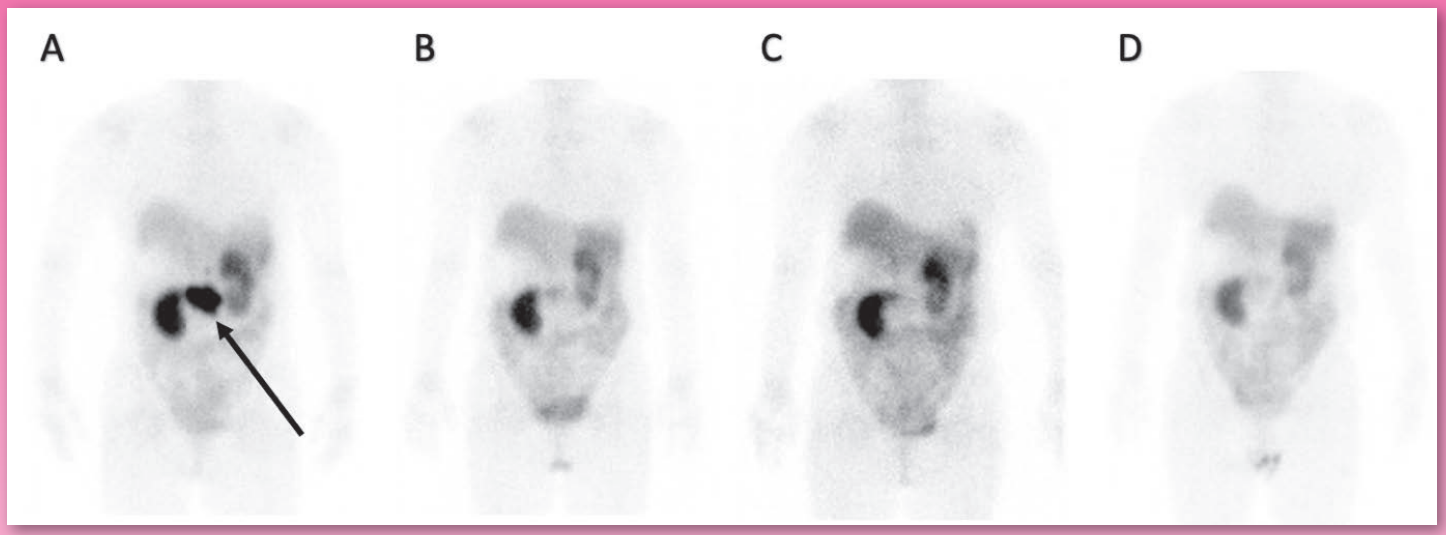

Post-treatment planar SPECT images acquired 24 hours after PRRT demonstrate a significant reduction in the primary tumor burden, with complete resolution of the main lesion observed when comparing images after the first and fourth treatments.(A) Planar SPECT image 24 hours after the first treatment showing radiotracer uptake in the pancreatic head tumor, mesenteric root, and mild heterogeneous uptake in the liver (arrow).(B) Planar SPECT image 24 hours after the second treatment showing a marked reduction in radiotracer activity in the pancreatic head tumor. (C) Planar SPECT image 24 hours after the third treatment.(D) Planar SPECT image 24 hours after the fourth treatment showing significantly reduced radiotracer uptake in the primary lesion.

Volume 21 Number 1 December 2024
第二十一卷 第一期 中華民國一一三年十二月
Published by NM Technology Committee, the Society of Nuclear Medicine, R.O.C.
中 華 民 國 核 醫 學 學 會
醫 技 委 員 會 發行

Volume 21 Number 1 Pages 1-60 December 2024

核醫技術學雜誌
Journal of Nuclear Medicine Technology

核醫技術學雜誌

第 21 卷第 1 期　中華民國核醫學學會醫技委員會學誌　中華民國 113 年 12 月發行

原　著

病例報告

其　他

Journal of Nuclear Medicine Technology

The Official Publication of NM Technology Committee, the Society of Nuclear Medicine, R.O.C.

ISSN 1818-2712

Volume 21, Number 1 December 2024

Original Articles

Case Reports

Others

中華民國 93 年 11 月 20 日創刊

發　　行：中華民國核醫學學會
秘 書 處

理 事 長：王 昱 豐

醫技委員會
主任委員：陳 惠 萍

總 編 輯：王 秀 珊

執行祕書：龔 瑞 英

投稿信箱：susanwang@ndmctsgh.edu.tw

會　　址：112 台北市北投區石牌路二段 201 號
核醫部轉核醫學學會

電　　話：02-2875-7301#587

電子信箱：tsnm.tw@gmail.com

劃撥帳號：19781819

戶　　名：中華民國核醫學學會

印　　刷：宇晨企業有限公司 yuchen68@ms51.hinet.net

地　　址：台北市和平東路二段 151 號 6 樓

電　　話：(02) 27037667　傳真：27033381

Impact of Acquisition Modes on Z axial Signal to Noise Ratio Distribution in Positron Emission Tomography: Step and Shoot versus Continuous Bed Motion mode

Fashun Tsai, Tai-Lin Jiang, Lin-Chun Ou, Cheng-Hui Lee

Division of PET Center, Shin Kong Wu Ho-Su Memorial Hospital, Taipei, Taiwan

Abstract

Introduction: With the advancement of computer technology, 3D image acquisition has become a routine application of clinical PET/CT. The axial sensitivity profile of 3D scan shows a sharp peak, and the sensitivity of the central slice is higher than the sensitivity of the edge slices on both sides. Due to the different sensitivities of each slice, the signal to noise ratio (SNR) of each slice at the same acquisition time is also different, with the highly sensitive central slice having a higher SNR than the edge slices. Conventional whole-body PET scan uses Step and shoot (SS) mode, a 3D image acquisition mode that requires high inter-FOV overlap to achieve good axial SNR uniformity. Currently, Continuous bed motion (CBM) mode is introduced for clinical use. In order to evaluate the effect of CBM on the axial SNR performance, this experiment was performed using a homogeneous ^{68}Ge cylindrical source with a single-bed scan and a dual-bed scan to analyze the difference in the axial SNR performance.

Materials and Methods: A ^{68}Ge cylindrical source was placed in the center of a Siemens Biograph Vision 450 PET/CT scanner for single-bed and dual-bed scan. Conventional whole-body PET/CT scan parameters were used. Single-bed scan was performed at 1 min/bed, 3 min/bed, and 5 min/bed, and dual-bed scan was performed at 1 min/bed, 5 min/bed, and 1 min/bed + 5 min/bed, respectively. According to the conversion table, progressive single-bed scan was performed at 1.7 mm/sec, 0.6 mm/sec, and 0.3 mm/sec bed movement velocity, and CBM mode dual-bed scan was performed at 1.7 mm/sec, 0.3 mm/sec, and 1.7 mm/sec + 0.3 mm/sec, respectively. The 2D ROI values of each section were recorded by circling each group of PET images with different scan modes, and the signal to noise ratio was calculated. The slice signal to noise ratio was defined as ROI_{mean} /ROI_{std}.

Results: The distribution of the axial signal to noise ratio in a single-bed scan showed a central peak shape, which was consistent with theory. Regardless of the scan time or the bed movement speed, the SNR of the central slice was much better than that of the edge slice. The central slice SNR was about 8.9 times that of the edge slice for SS mode, and about 3.8 times that of the edge slice for CBM mode. CBM mode scan continuously showed better SNR than SS mode in all corresponding bed velocity and acquisition time groups. The results of dual-bed scan at different bed velocities or acquisition times also show that CBM mode also exhibits smoother SNR profile than SS mode.

Conclusion: This experiment demonstrated that the CBM mode may provide a more uniform Z axial SNR distribution than the SS mode.

Keywords: continuous bed motion, CBM, step and shoot, sensitivity profile, signal to noise ratio, SNR

J Nucl Med Tech 2024;21:1-11

Received 2024/7/12
Corresponding author: Fashun Tsai
Division of PET Center, Shin Kong Wu Ho-Su Memorial Hospital, Taipei, Taiwan
Address: No. 95, Wenchang Rd., Shilin Dist., Taipei City 111, Taiwan (R.O.C.)
Division of PET Center
E-mail: T005629@ms.skh.org.tw

Introduction

Early PET and PET/CT scanners were typically provided with septa to switch between 2D and 3D acquisition modes. Septa in a PET scanner are movable partitions, typically made of lead, that improve the image quality by controlling how gamma rays are detected. Acquisition with septa extended, 2D mode, only gamma rays traveling in a straight line between opposing detector rings are counted. In 2D mode, typically the data from crystals directly across from each other was accepted, defining a transaxial slice. The septa are typically designed to also accept LORs that cross one crystal width in the axial direction, and this defines a "cross-plane" slice[1-3]. This simplifies image reconstruction but reduces sensitivity septa block gamma rays that have scattered off internal organs before reaching the detectors. This reduces noise in the final image and improves its accuracy. Photons blocked by septa can only receive incident photon pairs at certain angles, limiting detecting sensitivity. The 3D acquisition mode without septa can receive more incident photon pairs, achieve higher sensitivity, and detect more random events. The 3D acquisition mode allows detection of more gamma rays, including those at oblique angles, leading to a more detailed and sensitive image. The axial sensitivity profile for 3D acquisition is determined geometrically and is a triangular function, peaked at the center of the field of view (FOV). The relative 2D acquisition mode's Z axial sensitivity profile resembles a trapezoid, with more constant sensitivity in the central section[1-4].

Higher slice sensitivity allows for more counts under the same conditions, reducing statistical noise and resulting in a higher signal to noise ratio (SNR)[5]. This means that in a single-bed scan, the center slice of the 3D mode will have a significantly greater SNR than the edge slice. Currently, the majority of PET scans are performed in oncology and require numerous scanner FOV data coupled to cover a wide section of the patient body. These Whole-Body PET studies are performed by translating the patient through the scanner and acquiring data at multiple bed positions. These scans are obtained by acquiring the data in step and shoot mode (SS mode) with some overlap in the axial direction in order to improve uniformity of axial sensitivity[1, 3, 6]. Considering the effect of the slice sensitivity profile, 3D acquisition mode requires larger FOV overlap than 2D mode to achieve Z axial homogeneity.

The step and shoot mode is characterized by the patient bed remaining stationary at each bed position for image acquisition and then moving to the next bed position after completing the acquisition of one bed position. In recent years, new PET/CT scanners from manufacturers have introduced Continuous bed motion (CBM) scan mode for clinical use[7, 8]. Unlike the step and shoot mode, the CBM mode allows the patient bed to move throughout the image acquisition process. The SS mode in the scan parameter settings determines the acquisition time, expressed in minutes, for each bed position. On the other hand, the CBM mode determines the patient bed's movement speed in millimeters per second (mm/s) for each scan section. Depending on the clinical requirements, modern PET/CT scanners can be configured to set varied acquisition durations for each segment or varying bed movement speeds.

To facilitate the understanding of the two scan modes and to gain experience with both techniques, this study will evaluate image quality using a standard radioactive source. We will investigate the effects of different bed movement speeds and bed position acquisition times. Additionally, single-bed and dual-bed scans will be performed with the default overlap range specified by the manufacturer. A conversion table provided by the manufacturer will be used to analyze the signal to noise ratio (SNR) differences between slices.

MATERIALS AND METHODS

All PET/CT scan data were acquired using a Biograph Vision 450 PET/CT scanner (Siemens Medical Solutions USA, Inc.). It contains 38 blocks per ring for six rings along the axial FOV. Each block is subdivided into 4 × 2 mini-blocks (four mini-blocks in tangential position for two mini blocks in the axial position), that each contain an array of 5 × 5 LSO crystals of 3.2 × 3.2 × 20 mm^2. The mini block is coupled to an

array of 16 × 16 mm^2 SiPMs. The scanner comprises 60 crystal element rings 820 mm in diameter with 760 crystal elements per ring, covering an axial FOV of 200 mm and a transaxial FOV of 700 mm. A 2.28mCi ^{68}Ge sealed source (Model:CS-27, Siemens Healthcare) with a length of 270 mm and a diameter of 200 mm was place in the center of scan field as photon source. The single-bed and dual-bed studies will be conducted in SS mode and CBM mode respectively. In the single-bed SS mode study, 1min/bed, 3min/bed, and 5min/bed scans were carried out; in the dual-bed SS mode study, 1min/bed, 5min/bed, and 1min/bed+5min/bed scans were carried out. The manufacturer's conversion table indicated that bed acquisition times of 1min/bed, 3min/bed, and 5min/bed corresponded to equivalent patient bed speeds of 1.7 mm/s, 0.6 mm/s, and 0.3 mm/s, respectively. Therefore, the single-bed CBM study used 1.7 mm/s, 0.6 mm/s, and 0.3 mm/s scans; the dual-bed CBM study used 1.7 mm/s, 0.3 mm/s, and 1.7 mm/s+0.3 mm/s scans. Image reconstruction parameters: image matrix of 440 × 440, OSEM3D with application of TOF and resolution modelling, 4 iterations, 5 subsets, and All-pass filtering. Following image reconstruction for each scan, a circular region of interest (ROI) with a diameter of approximately 18 cm was drawn on each image slice to extract pixel values for subsequent image SNR analysis. For each acquisition mode, the SNR of axial slices was calculated as the ratio of the mean value of ROI (ROI_{mean}) to the standard deviation of ROI (ROI_{std}).

RESULTS

For single-bed scan, a total of 66 slices were scanned, with the first and 66th slices defined as edge slices and the 33rd and 34th slices defined as central slices. The comparison of the mean SNR values of the central slice, the mean SNR values of the edge slices and the ratio of the SNR of the central section to the edge slices are shown in Table 2. In the CBM mode, the SNR ratio between the central and edge slices is around 3.8, whereas in the SS mode, it is around 8.9.

Figures 1 to 3 show the experimental results of single-bed SS mode and single-bed CBM mode scan. The abscissa is the relative distance between each slice and the central slice, and the zero point of the abscissa is the center of the ^{68}Ge source.

Table 1. Conversion table for the Biograph Vision 450 PET/CT scanner showing the mapping of step and shoot min/bed acquisition time to patient bed flow velocity for equivalent image quality.

Step and shoot acquisition time (min/bed)	Patient bed flow velocity (mm/sec)
1	1.7
2	0.9
3	0.6
4	0.4
5	0.3
8	0.2

Table 2. The results of single-bed scan tests, along with central slice SNR_{mean}, edge slice SNR_{mean}, and center-edge-slice SNR_{mean} ratios for various scan parameters, are presented in this table.

Single-Bed scan		SNR_{mean} for central slices	SNR_{mean} for edge slices	SNR_{mean} ratio (central slice/edge slice)
Step and shoot	1min/bed	9.59	1.01	9.45
	3min/bed	16.11	1.83	8.82
	5min/bed	21.35	2.40	8.90
Continuous bed motion	1.7mm/sec	10.06	2.59	3.88
	0.6mm/sec	16.62	4.27	3.89
	0.3mm/sec	23.35	6.14	3.80

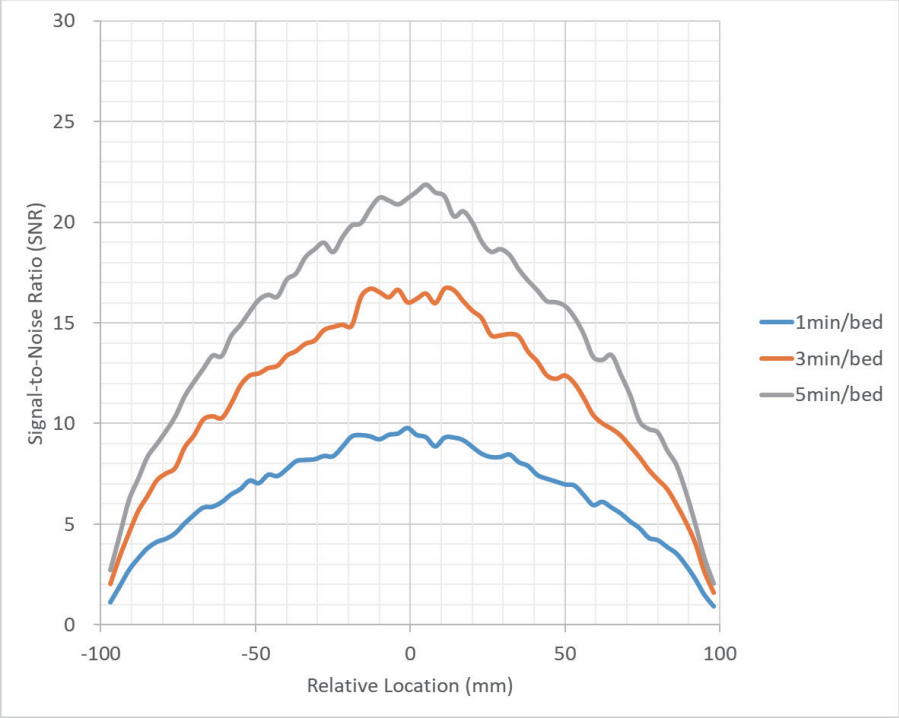

Figure 1. Signal to noise ratio for various emission time scans in single-bed SS mode scans. The Z axial SNR profile like a peak shape, central slice shows much higher SNR than edge slice.

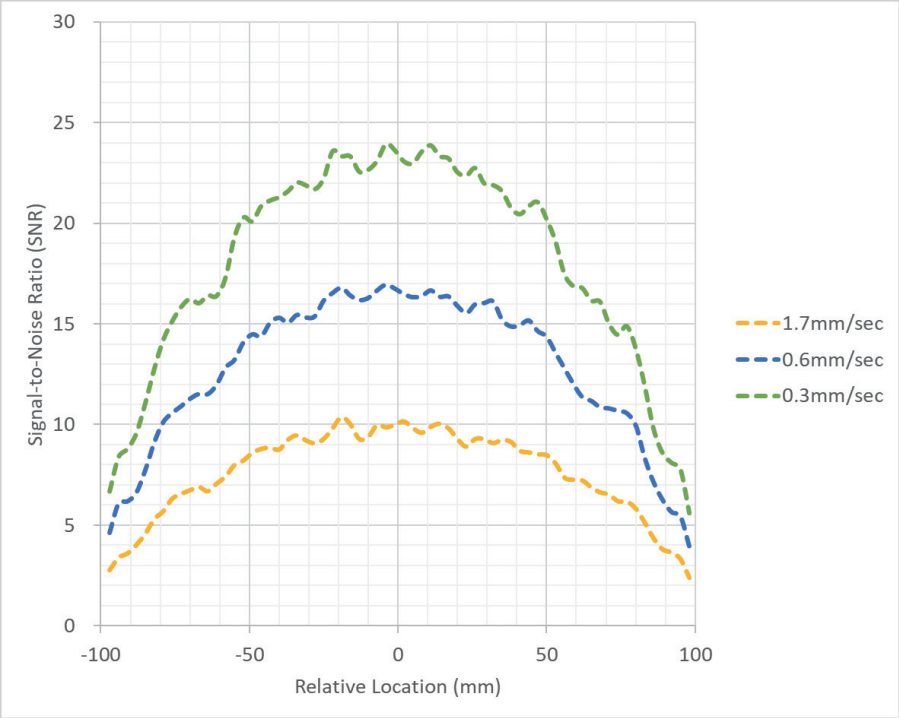

Figure 2. The Z axial SNR distribution curve for the single-bed CBM mode scan is rather mild. There is no evident dramatic top, and the center section is a plateau area.

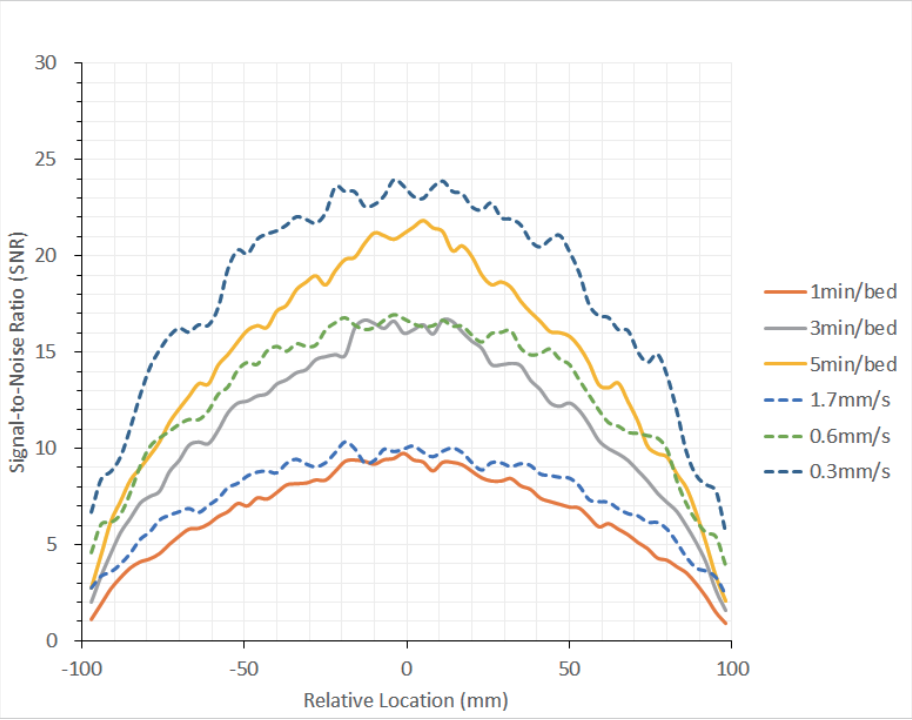

Figure 3. When comparing the SNR distribution curves of SS mode and CBM mode, the SNR performance of the edge area in CBM mode is clearly superior to that of SS mode.

Figure 4 and Figure 5 illustrate the test results for dual-bed scan. Figure 4 depicts the results of dual-bed scan with identical speed and time, where the acquisition time or bed velocity is constant for both the first and second bed positions. The results displayed in Figure 4 indicate that the CBM mode continues to exhibit higher SNR and SNR uniformity than SS mode scan across all regions in the Z axis. The radioactive range of the ^{68}Ge source has a length of 270 mm. Due to this limitation, only experimental data acquired within a ±135 mm range from the source center are presented and discussed in this work.

In modern PET/CT scanners, multi-bed acquisitions allow for the configuration of distinct scan durations for each bed position, tailoring the examination to specific clinical needs. Figure 5 presents the results of a dual-bed scan experiment investigating the impact of varying acquisition times and bed speeds. Notably, the step and shoot mode employed a 94 mm overlap between the two bed positions (±47 mm), with scan distances of 196 mm for the single-bed scan and 298 mm for the dual-bed scan. In CBM mode, a predetermined scan range is established for each bed velocity. In the dual-bed experiment, the point of transition between the two distinct bed motion rates is located at coordinates 0, corresponding to the Z axial center of the ^{68}Ge source.

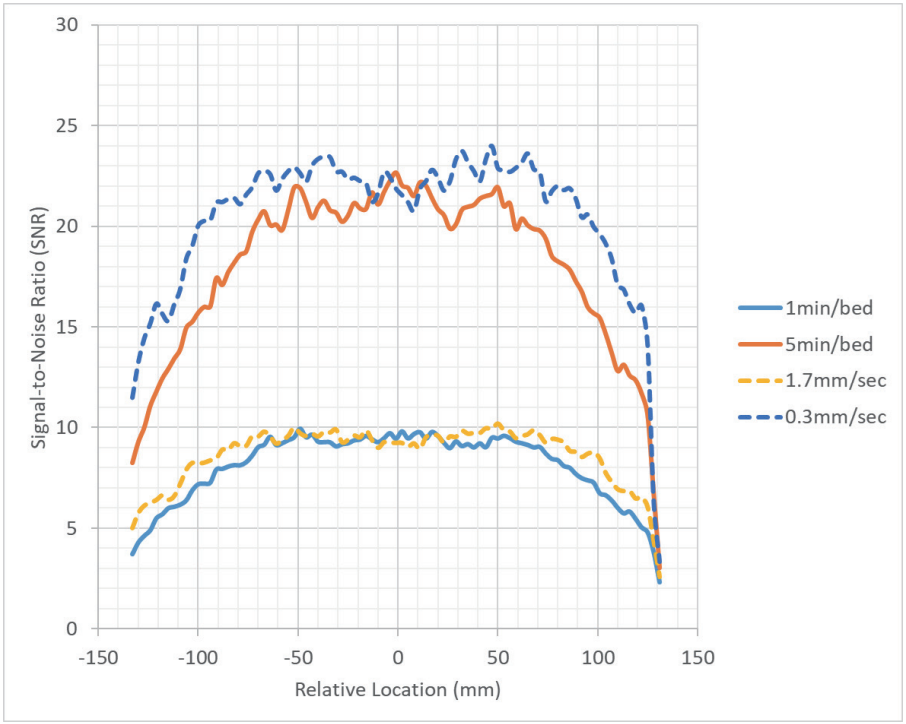

Figure 4. Dual-bed scan with constant bed velocity and acquisition time. The overlap between neighboring bed positions in SS mode scan makes it easier to create a gently sloping plateau area with consistent SNR characteristics. But the CBM mode provides a uniform SNR distribution over an even larger plateau area.

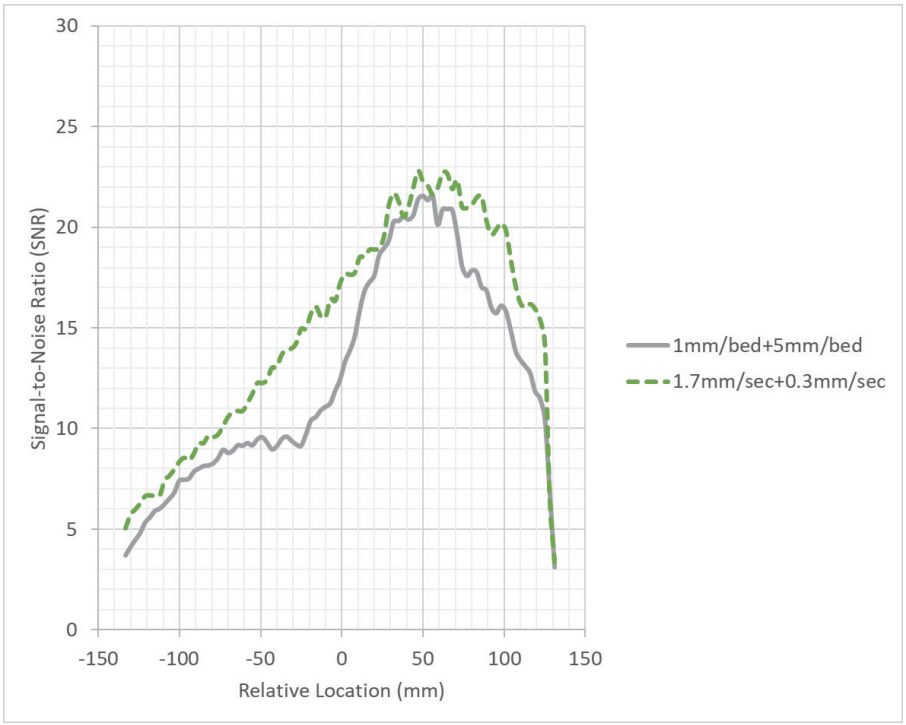

Figure 5. Dual-bed scan with varying bed speeds and acquisition durations. The SNR curve in the transition area of two bed sections with varied scan parameters demonstrates that CBM scan can result in a smoother transition.

DISCUSSION

The step and shoot whole-body acquisition approach has been the standard for data collection since the inception of PET. Continuous bed motion is an additional PET acquisition technique that was first reported by Dahlbom et al. in 2000 and evaluated by Brasse et al. in 2002[8, 9]. When doing a scan with CBM technology, technologists must think differently. The term “bed position”, which refers to a single field of view, is not used unless the scanner is set up for traditional acquisition methods. The overall scan duration in classic SS mode is calculated by multiplying the number of minutes per bed position by the total number of bed positions required to cover the desired axial range. The CBM mode uses just bed speed and axial range to determine scan time. If more counts are required with an SS mode image, the technologist increases the number of minutes each bed position; however, with CBM mode, the inverse occurs, and bed speed is reduced to increase the number of counts in the acquisition. The conversion table provided by the manufacturer for acquisition time and patient bed velocity is shown as a conversion curve in Figure 6. It is a non-linear proportional conversion, which requires operators to take time to adapt. The findings of our experiment demonstrate that the manufacturer's acquisition time to bed rate conversion table may provide equivalent SNR distributions in the two modes.

The most apparent distinction between SS mode and CBM mode is the manner in which the bed is positioned during the acquisition process. In the traditional approach employed with an SS mode PET scanner, the table remains stationary for the selected bed position, after which it abruptly transitions to the subsequent bed position. This is the origin of the term "step and shoot". Patients undergoing scan procedures are subjected to a series of physical stimuli, including multiple accelerations, movements, and sudden stops, which can result in discomfort. Subsequently, the bed positions are merged to create a comprehensive image of the entire body. During whole-body PET acquisitions using CBM mode, the table remains in continuous motion throughout the selected axial range. A study of patient preferences between

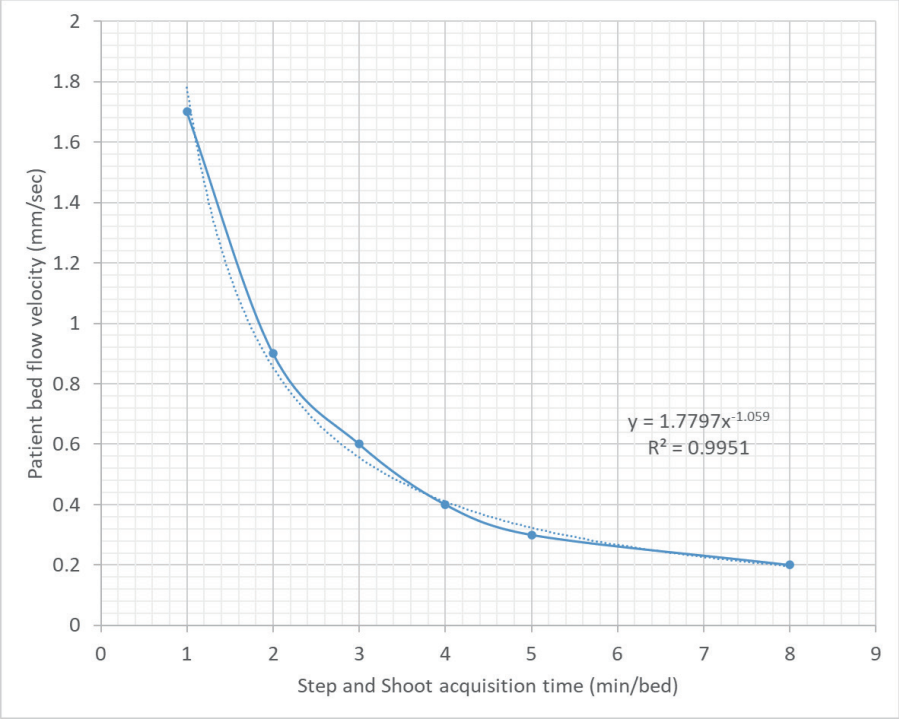

Figure 6. The conversion curve provided by the manufacturer for acquisition time and patient bed velocity. It approximates a power function curve.

SS and CBM modes revealed a substantial preference for CBM mode. This was found to be more relaxing, silent, and smooth than scan with SS technology[10].

In clinical PET scan practice, the CBM mode gives the technician a new option to configure the scan range to a continuous range similar to a CT scan, eliminating the need for individual PET bed positions. Frequently, a technologist finds that they require a little bit more coverage for the PET FOV and that they must include the whole bed position in the acquisition procedure. Due to the need to extend the CT range to meet the PET FOV, this additional position lengthens scan times and exposes users to additional radiation. The CBM mode enables the scan length to be optimized, which in turn reduces the radiation dose received by the patient during the PET/CT scan[11].

In conventional PET/CT image interpretation, nuclear medicine physicians extend their analysis beyond the transaxial plane, incorporating sagittal and coronal reconstructions for a more holistic assessment[3, 6]. However, a significant challenge arises due to the non-uniform distribution of SNR along the Z-axis. As depicted in Figure 7, SNR demonstrably exhibits a marked decrease at the superior and inferior extents of the sagittal and coronal slices, potentially compromising the evaluation of lesions residing in these peripheral regions. The data from this experiment indicate that the SNR performance of the edge section in CBM mode is more consistent with that of the central section. This may provide nuclear medicine physicians with greater confidence in their assessments. According to research by Osborne et al. and Rausch et al., physicians preferred the CBM approach over the SS mode[7, 11]. The quantification and picture quality of end surfaces were statistically considerably enhanced in both trials using the CBM approach.

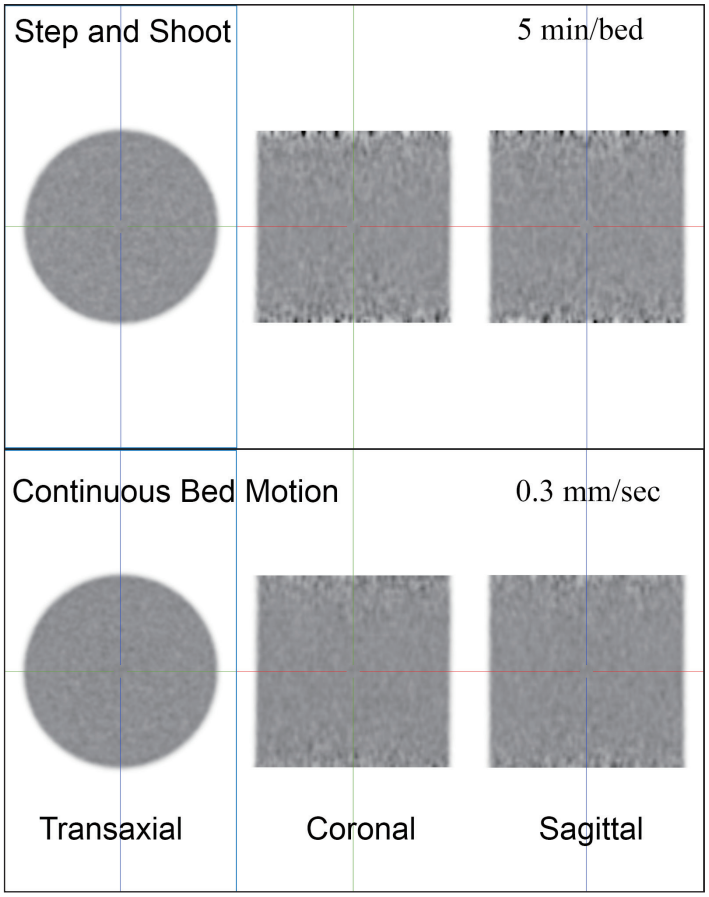

Figure 7. Transaxial, coronal and sagittal views of step and shoot mode and continuous bed motion mode scan.

The SNR of a PET image is positively correlated with the number of photon counts. Theoretically, to obtain the original N times SNR value, N-square times the number of photons or a corresponding increase in acquisition time is required[1, 5]. If the SNR measurement value under the SS mode 1 min/bed in single-bed is used as the standard, the theoretical SNR values of 3 min/bed and 5 min/bed are shown in Figure 8. Obviously, it can be seen that the curves of 3 min/bed and 5 min/bed SNR theoretical values and the actual measured values are highly coincident, which confirms that the theory is valid. Evaluating the data in Table 2, the SNR_{mean} of the edge slice in the single-bed CBM mode with 1.7mm/sec is 2.59, which is about 2.56 times of the SNR_{mean} of 1.01 for the corresponding SS mode with 1 min/bed. Theoretically, it takes 2.562 times the acquisition time in single-bed SS mode, which is about 6.55 min/bed, for the SNR value of the edge slice to be comparable to that of the CBM mode. In a single-bed scan: SS mode 1 min/bed consumes 1 min, CBM mode 1.7 mm/sec consumes 1 min 55sec. However, it takes 6.55 min in SS mode for the SNR of the edge slice to approach the SNR of the edge slice in CBM mode 1.7 mm/sec. This could be advantageous in short-distance localized scans for clinical application.

The standard uptake value (SUV) is a way of assessing PET scans that is subject to variance due to technical variables of the scanner system and patient characteristics[3, 6]. There are two commonly used techniques to SUV: the mean of all voxels inside the ROI (SUV_{mean}) and the maximum SUV (SUV_{max}). The SUV_{mean} includes data from many voxels, making it less susceptible to image noise. However, the measured SUV_{mean} will change based on the voxels included in the mean, making it susceptible to ROI definition and influenced by differences in ROI sizes among observers. The SUV_{max}, representing the maximum voxel value within the ROI, is more susceptible to noise than other SUV values. However, it has no impact on the definition of the ROI[12-15]. The findings of the experiment indicate that the CBM mode exhibits a more uniform Z-axis SNR profile than the SS mode. This results in a more consistent SUV_{max} quantification.

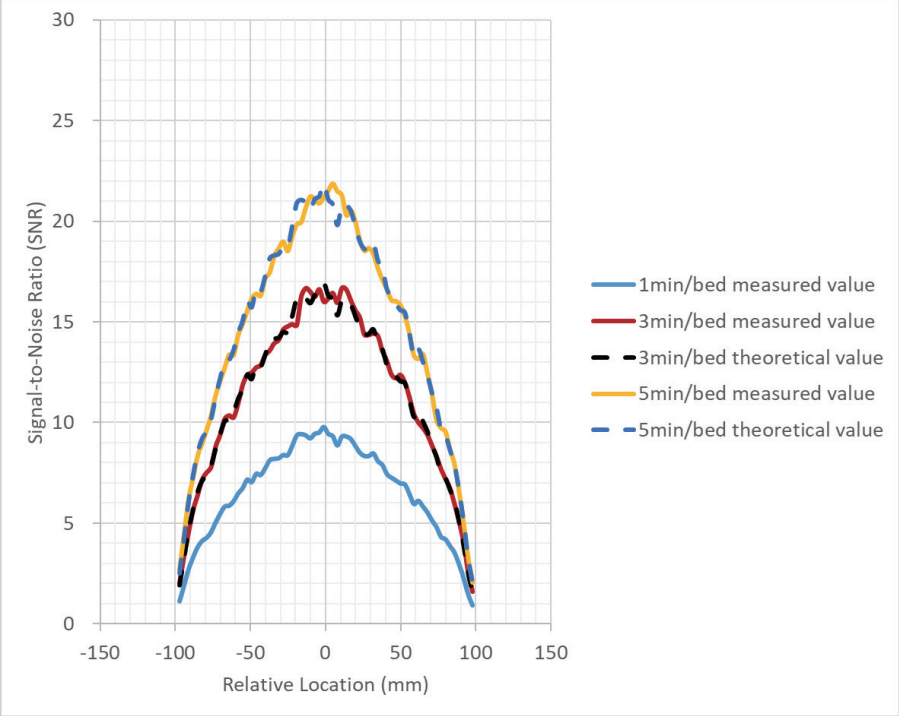

Figure 8. Comparison of SNR theoretical and actual measurement values.

CONCLUSION

The results of this study indicate that CBM mode can offer superior image SNR performance and Z-axis SNR consistency than SS mode in single-bed or dual-bed PET scan. It is theoretically possible for the CBM mode to have superior quantitative performance of SUV_{max}. However, converting the length of patient bed advancement per second from the traditional acquisition time for each bed position is a challenging process that requires a shift in thinking for staff, and it takes some time for them to become proficient in this method.◦

REFERENCES

1. Bailey, D.L., et al., *Positron Emission Tomography: Basic Sciences.* 2006: Springer London.
2. Bendriem, B. and D.W. Townsend, *The Theory and Practice of 3D PET.* 2013: Springer Netherlands.
3. Lawton, M.T., et al., *PET and PET/CT: A Clinical Guide.* 2005: Thieme Medical Publishers.
4. Sharma, S.D., et al., *Whole-body PET acceptance test in 2D and 3D using NEMA NU 2-2001 protocol*. Journal of Medical Physics, 2007. 32(4): p. 150-155.
5. Dougherty, G., *Digital Image Processing for Medical Applications.* 2009: Cambridge University Press.
6. Valk, P.E., et al., *Positron Emission Tomography*: Clinical Practice. 2006: Springer London.
7. Rausch, I., et al., *Performance evaluation of the Biograph mCT Flow PET/CT system according to the NEMA NU2-2012 standard.* EJNMMI physics, 2015. 2: p. 1-17.
8. Brasse, D., et al. *Continuous bed motion acquisition on a whole body combined PET/CT system.* in 2002 IEEE nuclear science symposium conference record. 2002. IEEE.
9. Dahlbom, M., J. Reed, and J. Young. *Implementation of true continuous 2D/3D whole body PET scanning. in 2000 IEEE Nuclear Science Symposium. Conference Record (Cat. No. 00CH37149).* 2000. IEEE.
10. Schatka, I., et al., *A randomized, double-blind, crossover comparison of novel continuous bed motion versus traditional bed-position based whole body PET/CT.* 2015, Soc Nuclear Med.
11. Osborne, D.R., et al., *Quantitative and qualitative comparison of continuous bed motion and traditional step and shoot PET/CT.* American Journal of Nuclear Medicine and Molecular Imaging, 2015. 5(1): p. 56.
12. Lucignani, G., *SUV and segmentation: pressing challenges in tumour assessment and treatment.* European journal of nuclear medicine and molecular imaging, 2009. 36: p. 715-720.
13. Benz, M.R., et al., *Treatment monitoring by 18F-FDG PET/CT in patients with sarcomas: interobserver variability of quantitative parameters in treatment-induced changes in histopathologically responding and nonresponding tumors.* Journal of Nuclear Medicine, 2008. 49(7): p. 1038-1046.
14. Brendle, C., et al., *Is the standard uptake value (SUV) appropriate for quantification in clinical PET imaging?–Variability induced by different SUV measurements and varying reconstruction methods.* European journal of radiology, 2015. 84(1): p. 158-162.
15. Adams, M.C., et al., *A Systematic Review of the Factors Affecting Accuracy of SUV Measurements.* American Journal of Roentgenology, 2010. 195(2): p. 310-320.

步進式與連續移動式掃描對於正子斷層 Z 軸向信雜比分布的影響評估

柴發順　江泰林　歐玲君　李正輝

新光吳火獅紀念醫院 正子造影中心

中文摘要

前言

隨著電腦科技的進步，3D 影像擷取模式已經是臨床 PET/CT 的常規應用。3D 掃描的軸向敏感度輪廓 (axial sensitivity profile) 呈現尖峰狀，中央切面的敏感度比兩側終端切面敏感度高。由於各切面的敏感度不同，相同收取時間下個切面的信雜比 (signal to noise ratio, SNR) 也不同，高敏感度的中央切面的信雜比會高於終端切面。傳統正子造影全身掃描採用步進式掃描 (step and shoot)，3D 影像擷取模式必須採用較高的床段間重疊才能獲得要好的軸向均勻度。目前連續移動式掃描 (continuous bed motion, CBM) 引入臨床使用。爲評估連續移動式掃描對於軸向信雜比的影響，本實驗利用均勻 ^{68}Ge 放射源假體，進行單一床段和雙床段掃描，分析 Z 軸向切面信雜比的差異。

材料與方法

將 ^{68}Ge 圓柱狀放射源置於 Siemens Biograph Vision 450 PET/CT 掃描儀中心進行單一床段和雙床段掃描。採用常規全身 PET/CT 掃描條件進行。分別以每床段 1 分，3 分鐘，5 分鐘進行步進式單一床掃描；以每床段 1 分，5 分鐘，1+5 分鐘進行步進式雙床掃描。依據時間對速度換算表進行換算，分別以 1.7mm/sec，0.6mm/sec 和 0.3mm/sec 的檢查床移動速度進行連續移動式單一床掃描；以 1.7mm/sec，0.3mm/sec，1.7mm/sec + 0.3mm/sec 進行連續移動式雙床段掃描。各組不同掃描模式的 PET 影像，圈選記錄各切面的 2D ROI 數值，並計算信雜比。定義切面信雜比爲 ROI_{mean} /ROI_{std}。

實驗結果

單一床段軸向信雜比分布呈現中央高峰形狀，與理論相符合。無論採用多掃描時間或床板移動速度，中央切面的信雜比皆遠優於邊緣切面。步進式掃描中央切面信雜比約爲邊緣切面的 8.9 倍，連續移動式掃描中央切面信雜比約爲邊緣切面的 3.8 倍。在各個對應速度與時間的組別中連續移動式掃描接表現出比步進式掃描更好的信雜比。不同速度或掃描時間條件下雙床段掃描結果也顯示出連續移動式掃描也顯示更平順的信雜比過度。

結論

本次實驗結果反應連續移動式掃描確實能提供較爲均勻的 Z 軸向信雜比分布。

關鍵字：正子斷層造影、步進式影像擷取、連續移動式影像擷取、軸向敏感度輪廓、信雜比

核醫技學誌 2024;21:1-11

接受日期：2024 年 7 月 12 日
通訊作者：柴發順
聯絡地址：台北市士林區文昌路 95 號新光吳火獅紀念醫院正子造影中心
電子郵件：T005629@ms.skh.org.tw

大腸蠕動檢查

鄭雯文[1]　杜高瑩[2]

馬偕紀念醫院 核醫科
[1]淡水院區
[2]台北總院

摘要

便祕是目前常見的文明病之一，辨別原發性或次發性〈器質性〉的便秘後，才能對症下藥。1999 年，Dylan Bartholomeuse 等人進行 Ga-67 與 In-111 的比較，發現其兩者結果大同小異，這對台灣的核醫科來說是件好消息，因爲 Ga-67 的取得與價錢都會比 In-111 來的方便及便宜，因此本科評估數值也是參考此篇研究結論。本科臨床作業流程是請病人口服 300c.c. 混有 1mCi Ga-67 的白開水或柳橙汁、在第 6、24、48 及 72 小時進行造影。回顧 2020 ～ 2024 年的病人，總共有 33 名患者來本科做大腸蠕動檢查，年紀介於 20 ～ 73 歲〈平均年紀爲 42.97 歲〉，正常的患者 13 位、平均半清除時間爲 21.33 小時，異常患者有 20 位、平均半清除時間爲 75.22 小時；其中有 3 位因 72 小時候輻射量排出過少而無法計算半清除時間。從正常病患的影像中可以看到放射性同位素在大腸的活動狀況，升結腸〈Ascending Colon，A〉在第 6 小時可以顯影、72 小時後幾乎已無放射性殘留；橫結腸〈Transverse Colon，T〉與降結腸〈Descending Colon，D〉大約顯影時間爲 24 ～ 48 小時、乙狀結腸〈Sigmoid Colon，S〉與直腸〈Rectum，R〉顯影時間爲 24 ～ 72 小時。

關鍵詞：便祕、大腸蠕動檢查、鎵 -67

核醫技學誌 2024;21:13-19

接受日期：2024 年 6 月 26 日
通訊作者：鄭雯文
聯絡地址：(25160) 新北市淡水區民生路 45 號
聯絡電話：(02)2809-4661 分機 2299
電子郵件：chengwwnike@yahoo.com.tw

前　言

便祕是目前常見的文明病之一，造成便秘的原因很多，有可能是某些疾病的前兆、例如：腫瘤或腸躁症。根據統計，台灣有超過 500 萬人有便秘困擾、20 ～ 50 歲民眾近 25% 有便秘問題；65 歲以上民眾的比例更高達 4 成，一年吃超過 4 億顆軟便藥。〔1〕女性占大多數，但男性甚至小孩、老人都會發生。因此，辨別原發性或次發性〈器質性〉的便秘後，才能對症下藥。便祕的一般理學檢查有糞便檢驗等等，但一般檢查卻無法診斷腸道的蠕動狀況，必須透過大腸鏡或 X 光、核醫檢查；而核醫的檢查較無侵入性、輻射劑量低，且能提供生理功能影像及數據，可以讓醫師更了解病患的狀況。

國外最開始是 1962 年、用 Cr-51 來做腸道蠕動檢查〔2〕，第一份完整的全腸道蠕動評估是 1985 年，此研究是用 ^{111}In-DTPA，之後也是使用 In-111 居多〔3〕。1999 年，Dylan Bartholomeuse 等人進行 Ga-67 與 In-111 的比較，發現其兩者結果大同小異〔4〕，這對台灣的核醫科來說是件好消息，因爲 Ga-67 的取得與價錢都會比 In-111 來的方便及便宜，因此本科評估數值也是參考此篇研究結論。加上 Ga-67 經口服用之後，不易被腸胃道的其他器官吸收且最後是經由腸道排出，其物理半衰期爲 78.3 小時，非常適合用來評估腸道蠕動情況。

方法

本科的臨床標準作業流程是參考美國核醫學與分子影像協會〈The Society of Nuclear Medicine and Molecular Imaging，SNMMI〉及歐洲核子醫學會〈The European Association of Nuclear Medicine，EANM〉而擬定的〔5〕。病人接受檢查的前一天開始不能服用軟便劑，檢查前需禁食禁水 8 小時、當天會請病人口服 300c.c. 混有 1mCi Ga-67 的白開水或柳橙汁、在第 6、24、48 及 72 小時進行造影。病人服用造影劑之後，可以正常飲食，但

不能服用任何可能會促進腸道蠕動的藥物。影像收集系統是使用奇異公司的 Infinia Gamma camera 搭配中能量一般目的準直儀〈Medium Energy General Purpose，MEGP〉、能峰設定在 93、184 及 300keV〈能窗設定 ±26%、±20% 及 ±20%〉、矩陣大小〈matrix size〉爲 128×128，以靜態掃描方式收集前後腹部影像 10 分鐘。

影像分析方式是採用活度曲線湊合方法〈curve fitting〉，將第 6 小時收集的影像當作 100%，其餘 3 天依排出的輻射量進行活度曲線湊合去計算半清除時間〈half-clearance time〉。因爲 Ga-67 的物理半衰期爲 78.3 小時，所以在計算時也必須考慮本身的半衰期。

分析

本研究回溯統計自 2020 年 9 月至 2024 年 5 月來本科進行大腸蠕動檢查的病患。

結果與討論

回顧 2020 ～ 2024 年的病人，總共有 33 名患者來本科做大腸蠕動檢查，年紀介於 20 ～ 73 歲〈平均年紀爲 42.97 歲〉，正常的患者 13 位、平均半清除時間爲 21.33 小時，異常患者有 20 位、平均半清除時間爲 75.22 小時；其中有 3 位因 72 小時候輻射量排出過少而無法計算半清除時間，還有 1 位患者因私人理由沒有完成掃描，如表 1。

其中，女性患者有 29 位、年紀介於 20 ～ 73 歲〈平均年齡 40.31 歲〉；男性只有 4 名、年紀介於 39～72 歲〈平均年齡 62.23 歲〉，如圖 1。在 29 名女性患者中，有 1 名患者因私人理由沒有完成掃描，故無法分析；然而，有 11 名患者爲正常、半清除時間介於 11 ～ 26.9 小時；有 3 名受檢患者再經過 72 小時後，排出的輻射量太少導致無法計算，累積在乙狀結腸或直腸。其餘 14 名異常患者的半清除時間介於 33.2 ～ 652.3 小時〈平均半清除時間爲 112.4 小時〉。在僅有的 4 名男性患者，結果正常者有 2 名、平均半清除時間爲 20.6 小時；另外 2 名異常患者平均半清除時間爲 38.05 小時，如表 2。

從影像學來判斷，正常的 11 位患者在 24 小時左右已經到達左半邊的大腸〈降結腸、乙狀結腸及直腸〉、速率略慢但還是在正常清除時間的 2 位在 48 小時左右到達，如圖 2；19 名異常患者在 72 小時仍有中度或重度殘餘的輻射量，如圖 3。圖 4 爲其中 1 名患者經由曲線湊合後計算出半清除時間爲 46.14 小時。從正常病患的影像中可以看到放射性同位素在大腸的活動狀況，升結腸〈Ascending Colon，A〉在第 6 小時可以顯影、72 小時後幾乎已無放射性殘留；橫結腸〈Transverse Colon，T〉與降結腸〈Descending Colon，D〉大約顯影時間爲 24 ～ 48 小時、乙狀結腸〈Sigmoid Colon，S〉與直腸〈Rectum，R〉顯影時間爲 24 ～ 72 小時，圖 5。13 位正常的患者在 24 ～ 48 小時左右就已經到達左半邊的大腸，其中有 11 位患者在 24 小時內就已完全排除〈平均時間爲 18.55 小時；女性爲 16.49 小時、男性爲 20.60 小時〉。其餘 2 位患者的平均半清除時間爲 26.89 小時。

結論

綜觀而論，便祕的確好發於女性而且不論哪個年齡層都有可能發生，圖 6。核子醫學在便秘的診斷中具有顯著優勢，可以爲臨床醫生提供重要的功能性訊息，從而更準確地識別便秘的病因並製訂相應的治療方案。隨著技術的進步和應用的普及，核子醫學有望在胃腸道疾病診斷中發揮更大的作用。

參考文獻

1. 新聞中心蔡經謙，早安健康。全台逾 500 萬人便祕，醫揭 5 種工作最易便祕！喚醒腸子 3 秘訣變超順 [online]。2023.9.11 Available from: https://www.edh.tw/article/34650。
2. Hansky J, Connell A M, Measurement of gastrointestinal transit using radioactive chromium. 1962, Gut 3:187-188
3. Hardy J G, Perkins A L, Validity of the geometric mean correction in the quantification of whole bowel transit. Nucl Med Commun 1985 6:217-224
4. Bartholomeusz Dylan, Barry E. Chatterton, Johan C. Bellen, Robert Gaffney and Andrew Hunter. Segmental Colonic Transit After Oral ^{67}Ga-Citrate in Healthy Subjects and Those with Chronic Idiopathic Constipation. J Nuci Med 1999 40:277-282
5. Alan H. Maurer (Chair), Michael Camilleri, Kevin Donohoe et al. The SNMMI and EANM Practice Guideline for Small-Bowel and Colon Transit 1.0*. J Nuci Med 2013 54(11):2004-2013

表一　2020~2024 年大腸蠕動檢查總人數及結果

人數	正常		異常	
	< 24 小時	25 ～ 28.8 小時	> 28.8 小時	無法估算
男 + 女	11	2	16	4
女	9	2	14	4[註]
男	2	0	2	0

[註] 有 1 名患者因私人理由沒有完成檢查

表二　2020~2024 年大腸蠕動檢查平均半清除時間

平均半清除時間	正常		異常
	< 24 小時	25 ～ 28.8 小時	> 28.8 小時
男 + 女	18.55	32.47	75.22
女	16.49	26.89	112.40
男	20.60		38.05

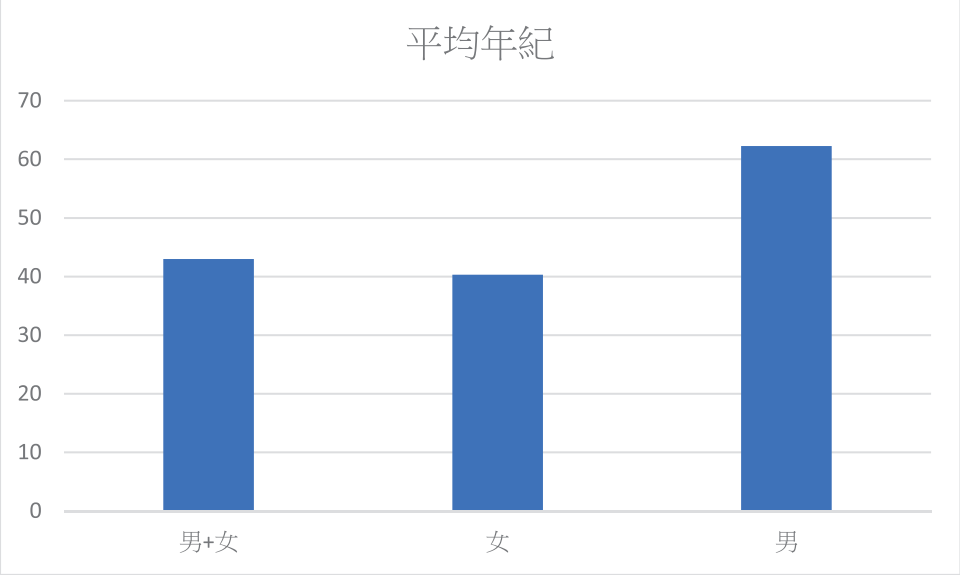

圖一　受檢病患的平均年齡

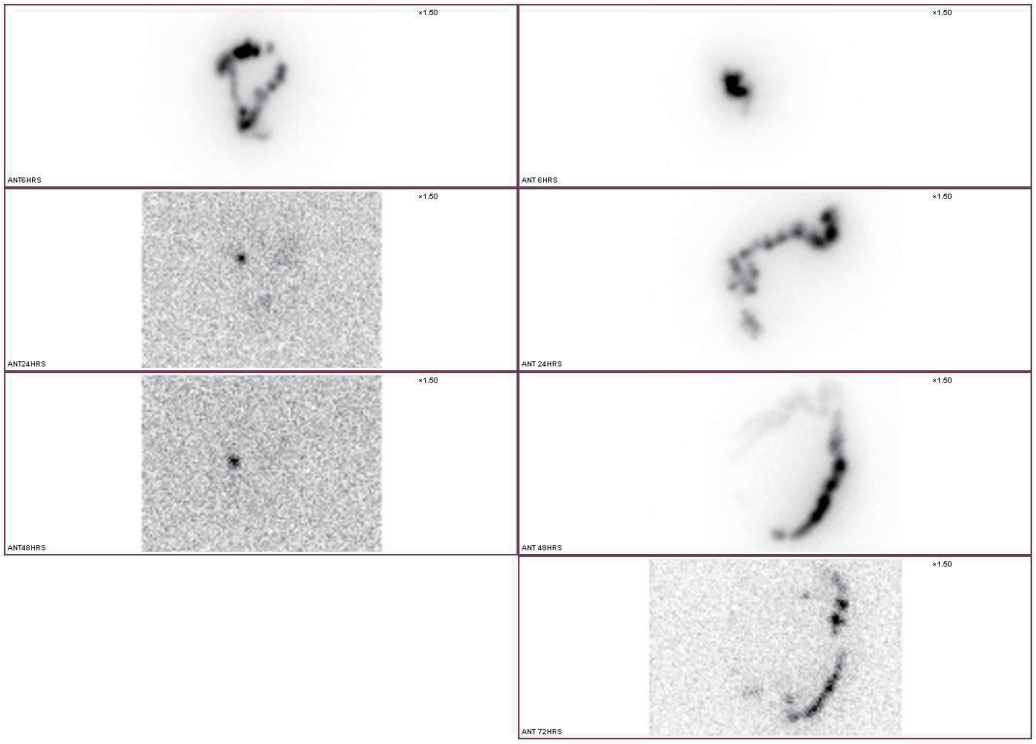

圖二 左右兩位爲正常患者。左半圖患者的半清除時間爲 15.5 小時，明顯看出 24 小時已排出大量的放射性藥物；右半圖患者的半清除時間爲 26.87 小時，在 72 小時的影像中可以看出殘餘的放射性藥物減少許多。

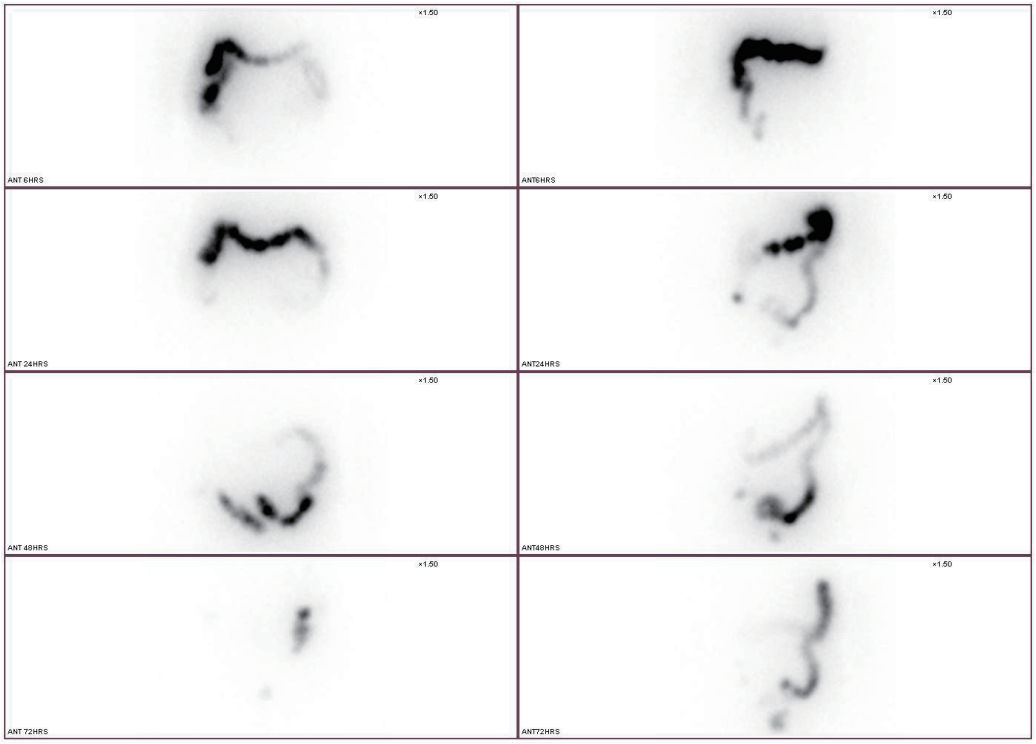

圖三 左右兩邊爲異常患者。左半圖患者半清除時間爲 46.14 小時，從影像可看出 72 小時後仍有中度殘留的放射性藥物；右半圖患者在 72 小時的影像可看出出有重度的放射性藥物殘留，故無法估算半清除時間。

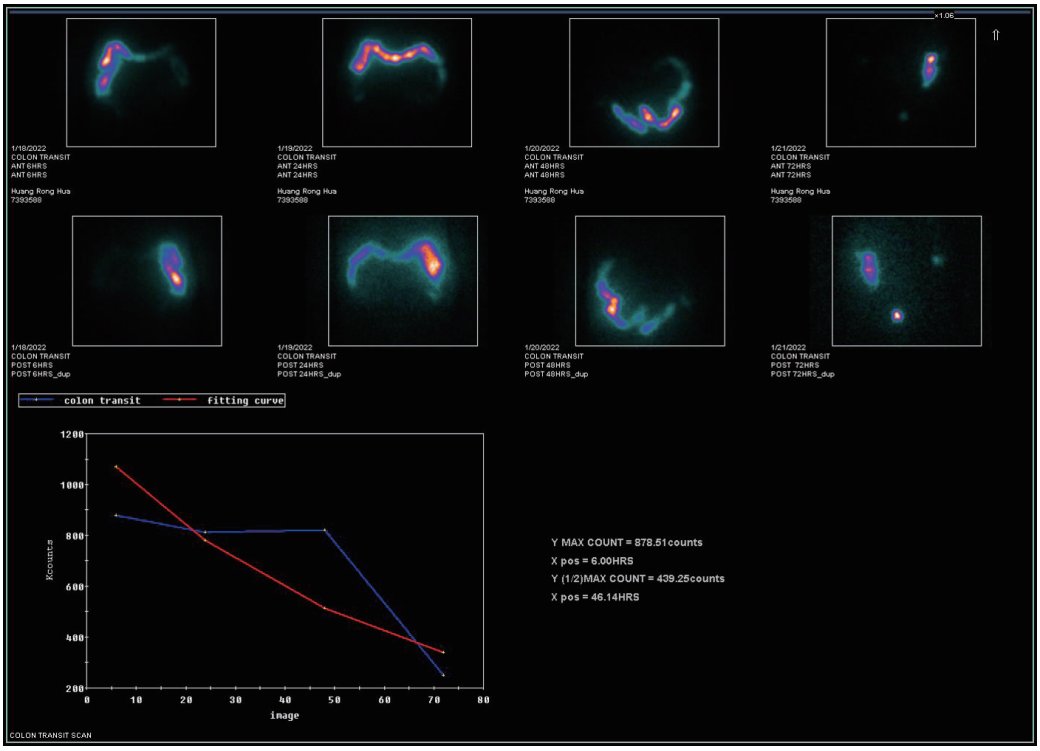

圖四　經過曲線湊合而得半清除時間爲 46.14 小時，此患者爲圖 3 左邊異常患者結果。

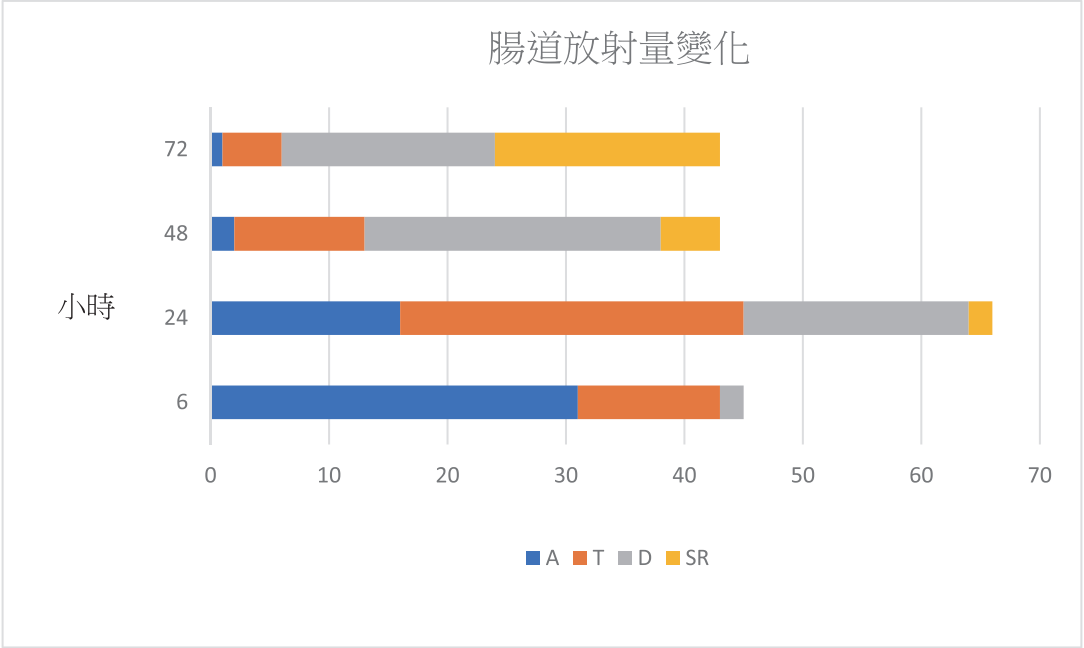

圖五　放射性同位素隨著時間在腸道的變化量

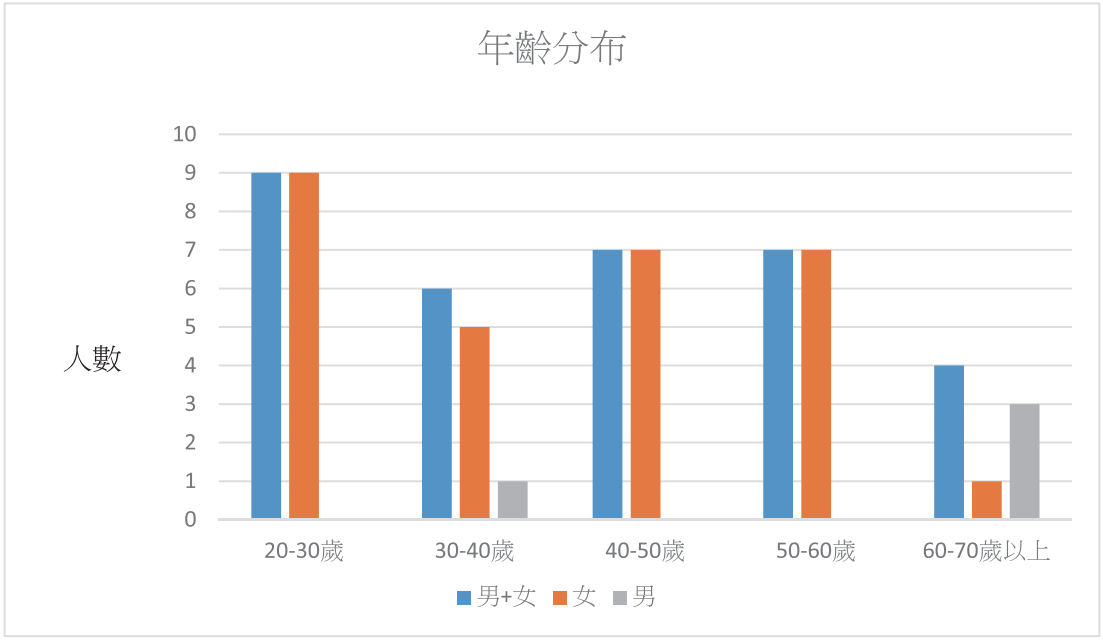

圖六 女性患者多於男性患者且可看出各個年齡層都有發生便秘的機率

Colon Transit Study

Wen-Wen Cheng[1], Kao-Yin Tu[2]

Department of Nuclear Medicine, MacKay Memorial Hospital
[1]Tamsui branch
[2]Taipei headsquares

Abstract

Constipation is one of the common modern diseases today. Distinguishing between primary and secondary (organic) constipation is essential for appropriate treatment. In 1999, Dylan Bartholomeuse et al. conducted a comparative study of Ga-67 and In-111, finding that the results of both were very similar. This is good news for Nuclear Medicine in Taiwan, as Ga-67 is more accessible and cheaper than In-111. Therefore, the evaluation metrics of our department also refer to the conclusions of this study. Our clinical procedure involves patients ingesting 300 c.c. of water or orange juice mixed with 1 mCi Ga-67, followed by imaging at 6, 24, 48, and 72 hours. Reviewing patients from 2020 to 2024, there were a total of 33 patients who underwent colon transit study in our department, ranging in age from 20 to 73 years (with an average age of 42.97 years). Among them, 13 were normal patients with an average half-clearance time of 21.33 hours, and 20 were abnormal patients with an average half-clearance time of 75.22 hours; 3 of these patients could not have their half-clearance time calculated due to insufficient radiation excretion after 72 hours. Imaging from normal patients showed the activity of the isotope in the colon: the ascending colon (A) became visible at 6 hours and had almost no radioactive residue after 72 hours; the transverse colon (T) and descending colon (D) were visible around 24 to 48 hours; and the sigmoid colon (S) and rectum (R) were visible from 24 to 72 hours.

Keywords: Constipation, Colon Transit Study, Ga-67

J Nucl Med Tech 2024;21:13-19

Received 2024/6/26
Corresponding author: Wen-Wen Cheng
Address: No.45, Minsheng Rd., Tamsui Dist., New Taipei City 251, Taiwan (R.O.C.)
Tel: (02) 2809-4661 ext.2299; E-mail: chengwwnike@yahoo.com.tw

Case Report on Peptide Receptor Radionuclide Therapy (PRRT) at a Teaching Hospital in a Specific Region

Wan-Jo Chang, Kuan-Yin Ko

Department of Nuclear Medicine of National Taiwan University Cancer Center, Taipei, Taiwan

Abstract

In the field of neuroendocrine tumor (NET) treatment, peptide receptor radionuclide therapy (PRRT) has emerged as a novel targeted therapeutic approach that has garnered widespread attention in recent years. PRRT leverages the characteristic overexpression of somatostatin receptors (SSTRs) on the surface of most NET cells. By combining the radionuclide Lutetium-177 with somatostatin analogs, this therapy enables precise targeting of tumor cells. This approach not only ensures effective delivery of radiopharmaceuticals to tumor sites but also minimizes damage to surrounding normal tissues, thereby enhancing therapeutic efficacy and reducing side effects.

The purpose of this study is to report a case from our hospital, emphasizing the integration of post-therapy single-photon emission computed tomography/computed tomography (SPECT/CT) imaging as part of the treatment evaluation process.

Keywords: Peptide Receptor Radionuclide Therapy (PRRT), Lutetium-177, Single Photon Emission Computed Tomography (SPECT/CT)

J Nucl Med Tech 2024;21:21-26

Received 2024/12/2
Corresponding author: Wan-Jo Chang
Address: B1F, No.57, Ln. 155, Sec. 3, Keelung Rd., Da'an Dist., Taipei City 106, Taiwan
Tel: 02-23220322#237954
E-mail: A01142@ntucc.gov.tw

Introduction

Neuroendocrine tumors (NETs) are a heterogeneous group of tumors originating from neuroendocrine cells. These tumors can occur in various organ systems, including the gastrointestinal tract, pancreas, and lungs. The clinical manifestations of NETs are diverse, ranging from asymptomatic cases to various endocrine symptoms caused by excessive hormone secretion. In recent years, advancements in diagnostic techniques have led to an increasing diagnosis rate of NETs, underscoring the urgent need for effective treatment strategies for this tumor type.

In the field of NETs treatment, Peptide Receptor Radionuclide Therapy (PRRT) leverages the characteristic overexpression of somatostatin receptors (SSTRs) on the surface of most NET cells. This approach combines the radionuclide Lutetium-177 (Lu-177) with somatostatin analogs to achieve precise targeting of tumor cells. PRRT not only efficiently delivers radiopharmaceuticals to the tumor site but also minimizes damage to surrounding normal tissues, enhancing therapeutic efficacy and reducing side effects.

Lu-177, a radionuclide that emits both gamma (γ) and beta (β) rays, offers dual functionality that is particularly advantageous in clinical settings for both diagnosis and therapy. Gamma (γ) rays enable imaging for treatment monitoring, while beta (β) rays effectively target and treat specific tumors. This dual capability allows for post-treatment imaging to observe tumor uptake and assess therapeutic efficacy. Therefore, we can collect post-treatment imaging to observe the tumor uptake status and evaluate the treatment effectiveness.

The radiopharmaceutical combining the radionuclide Lutetium-177 (Lu-177) with a somatostatin analog is known as 177Lu-DOTATATE. Currently, it is indicated for the treatment of unresectable or metastatic, progressive, and well-differentiated (G1 or G2) somatostatin receptor-positive neuroendocrine tumor patients.

The objective of this study is to report the treatment course of a neuroendocrine tumor patient at our hospital who underwent peptide receptor radionuclide therapy (PRRT) with 177Lu-DOTATATE and to evaluate the post-treatment imaging changes observed using Single Photon Emission Computed Tomography/Computed Tomography (SPECT/CT).

Case Report

The patient is a 66-year-old female diagnosed in 2021 with a neuroendocrine tumor of the pancreatic head. The tumor was staged as cT4N1M0, Stage III, with well-differentiated histology (Grade 1) and a Ki-67 index of less than 2%. Imaging studies revealed tumor invasion into the superior mesenteric artery and vein (SMA/SMV) as well as multiple metastatic lesions in the liver.

The patient previously underwent neoadjuvant chemotherapy with Avastin, DTIC, and 5-FU; targeted therapies with Everolimus and Sutent; and long-acting somatostatin analog therapy with Sandostatin. However, these treatments yielded limited efficacy. Subsequently, the patient was treated with peptide receptor radionuclide therapy (PRRT). Ga-68 DOTATOC PET scans and FDG PET scans were performed before and after the PRRT treatment to evaluate disease progression (Fig. 1).

Posttherapy Scan Acquisition

Whole-body planar and SPECT/CT imaging were performed 1 d after each cycle in the context of routine clinical care using a dual-head γ-camera NM/CT 870 DR (GE Healthcare) system with the following acquisition parameters: 208% ± 10% keV photopeak, 170% ± 10% keV scatter window, 128 × 128 matrix, 30 s per projection, 60 projections in total using 2 detectors, medium-energy general-purpose collimators, and a low-dose CT for attenuation correction. A Xeleris workstation (GE Healthcare) was used for reconstruction with the following reconstruction parameters: ordered-subset expectation maximization, 10 iterations, 6 subsets, and a Butterworth filter, with scatter correction and attenuation correction. The imaging duration was approximately 60 min, consisting of 1 whole-body planar acquisition and two 20-min SPECT/CT bed positions covering the kidneys and most of the tumor.

Treatment Course and Clinical Response

At our institution, peptide receptor radionuclide therapy (PRRT) was administered using a slow infusion method via an injection pump at a rate of 50 ml/hr. Each treatment session included antiemetic medication and amino acid infusions to protect renal function. The patient completed four treatment cycles, with the process and imaging findings summarized as follows:

- First Treatment: The injected dose was 187.9 mCi. Post-treatment whole-body and regional SPECT imaging showed that the radiotracer predominantly localized to the pancreatic head tumor and the mesenteric root, with mild heterogeneous uptake observed in the liver. Additionally, faint uptake in the left parietal bone was noted, raising suspicion of a possible lesion. At this stage, significant radiotracer uptake in the primary tumor confirmed the accuracy of treatment targeting.
- Second Treatment: The injected dose was 187.6 mCi. Compared with the first post-treatment imaging, the pancreatic head tumor demonstrated significantly reduced radiotracer activity. However, the faint uptake in the left parietal bone persisted, and the liver maintained mild heterogeneous activity.
- Third Treatment: The injected dose was 187.4 mCi. Imaging revealed further reduction in pancreatic tumor activity, with only minimal residual uptake. The left parietal bone lesion remained stable with no significant changes.
- Fourth Treatment: The injected dose was 183.9 mCi. Imaging showed stable activity in the pancreatic tumor with no new lesions or significant progression. The left parietal bone lesion continued to display faint activity,

suggesting a stable lesion. Comparison between the first and fourth post-treatment images revealed a marked reduction in uptake in the primary lesion (Fig. 2). Similarly, SPECT/CT imaging comparisons between the first and second treatments demonstrated a significant decrease in lesion uptake (Fig. 3).

Overall, pre- and post-treatment imaging (including PET and nuclear medicine scans) indicated a substantial reduction in tumor burden, with effective control of the primary tumor lesion and stable therapeutic outcomes.

Throughout the four treatment cycles, the patient exhibited mild bone marrow suppression, with good overall tolerability. However, prior to the final treatment, the patient's hemoglobin level dropped significantly to 8.7 g/dl, necessitating close monitoring for anemia and appropriate intervention (Table 1).

In summary, PRRT effectively reduced radiotracer activity in the patient's primary tumor lesion without causing significant treatment-related adverse events. This therapy demonstrated promising efficacy for the management of advanced pancreatic head neuroendocrine tumors, offering a viable clinical treatment option.

Conclusion

This case involved a patient with a pancreatic head neuroendocrine tumor (NET) who experienced disease progression despite multiple lines of prior treatments, including chemotherapy and targeted therapy. Following peptide receptor radionuclide therapy (PRRT) with Lu-177 DOTATATE, the primary tumor lesion showed a favorable therapeutic response. Whole-body imaging demonstrated a progressive reduction in lesion activity without evidence of new lesions.

Common side effects of Lu-177 DOTATATE include bone marrow suppression and mild renal function impairment. During the treatment course, the patient exhibited gradual declines in white blood cell count, hemoglobin, and platelet levels, culminating in mild anemia by the fourth treatment. However, this did not cause significant discomfort or interfere with the treatment process, indicating good overall tolerability.

Lu-177 DOTATATE is an effective treatment option for pancreatic head neuroendocrine tumors. This case illustrates its promising efficacy in advanced disease and supports further application and research in tumors with high somatostatin receptor (SSTR) expression. By sharing this case, we hope to provide a reference for the future promotion and clinical application of PRRT in Taiwan, ultimately enhancing treatment accessibility and quality of life for patients with advanced NETs.

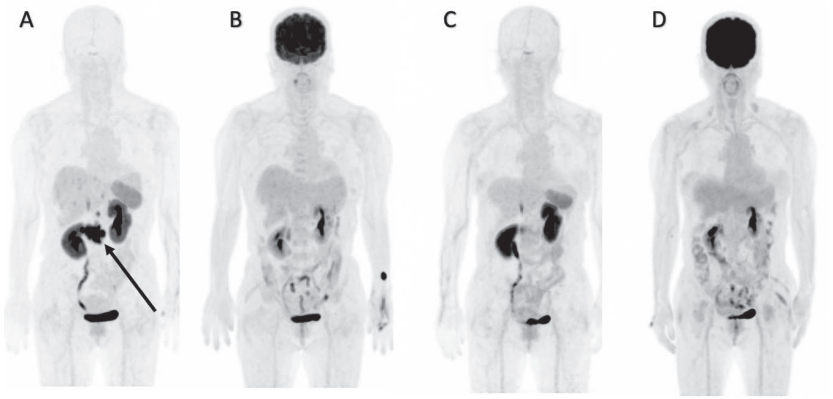

Figure 1. A 66-year-old female patient with a pancreatic head neuroendocrine tumor (NET), staged as cT4N1M0, Stage III, Grade 1, with multiple liver metastases. The patient underwent four cycles of 177Lu-DOTATATE treatment. Post-treatment imaging revealed a significant reduction in tumor burden, with effective control of the primary tumor lesion and stable therapeutic outcomes.(A) Pre-treatment 68Ga-DOTATATE PET/CT showing somatostatin receptor (SSTR)-positive disease (arrow).(B) Pre-treatment FDG PET/CT.(C) Post-treatment 68Ga-DOTATATE PET/CT showing resolution of lesions.(D) Post-treatment FDG PET/CT.

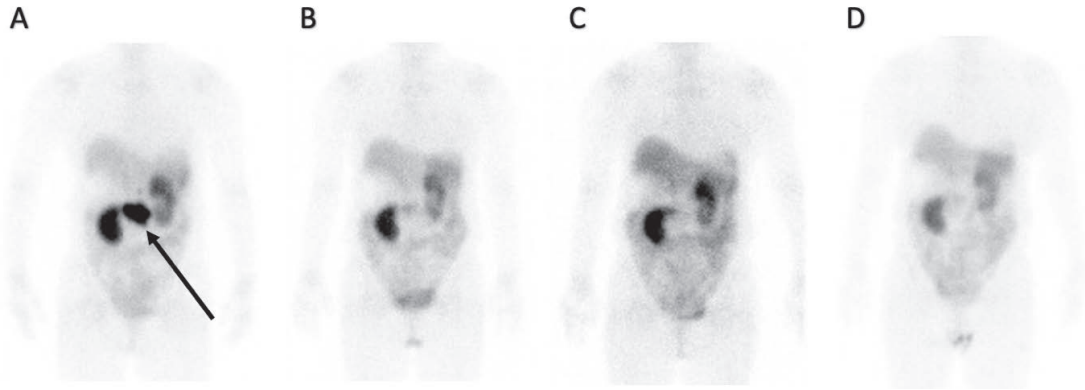

Figure 2. Post-treatment planar SPECT images acquired 24 hours after PRRT demonstrate a significant reduction in the primary tumor burden, with complete resolution of the main lesion observed when comparing images after the first and fourth treatments.(A) Planar SPECT image 24 hours after the first treatment showing radiotracer uptake in the pancreatic head tumor, mesenteric root, and mild heterogeneous uptake in the liver (arrow).(B) Planar SPECT image 24 hours after the second treatment showing a marked reduction in radiotracer activity in the pancreatic head tumor. (C) Planar SPECT image 24 hours after the third treatment.(D) Planar SPECT image 24 hours after the fourth treatment showing significantly reduced radiotracer uptake in the primary lesion.

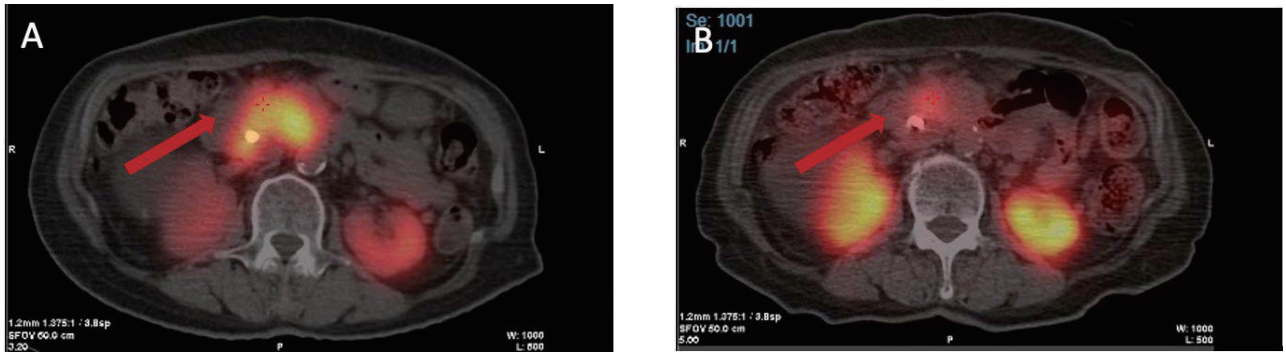

Figure 3. Post-treatment planar SPECT images acquired 24 hours after PRRT demonstrate a significant reduction in the primary tumor burden, with complete resolution of the main lesion observed when comparing images after the first and fourth treatments.(A) Planar SPECT image 24 hours after the first treatment showing radiotracer uptake in the pancreatic head tumor, mesenteric root, and mild heterogeneous uptake in the liver (arrow).(B) Planar SPECT image 24 hours after the second treatment showing a marked reduction in radiotracer activity in the pancreatic head tumor. (C) Planar SPECT image 24 hours after the third treatment.(D) Planar SPECT image 24 hours after the fourth treatment showing significantly reduced radiotracer uptake in the primary lesion.

Table 1. Hematological and Biochemical Reports for Each Treatment Session：

Treatment Session	WBC (/μL)	Hb (g/dL)	PLT ($\times 10^3$/μL)	Cre (mg/dL)	T-Bil (mg/dL)	Alb (g/dL)	AST (U/L)	ALT (U/L)
First Treatmet	6420	13.2	297	1.4	0.55	4.6	21	11
Second Treatmet	6930	12.9	371	1.0	0.70	4.2	27	17
Third Treatmet	4600	12.9	282	1.0	0.75	4.5	23	15
Fourth Treatment	3710	8.7	200	1.0	0.28	3.6	17	10

Hematological and Biochemical Report Notes

1. WBC：The patient's overall white blood cell count gradually decreased with each treatment session. Before the fourth treatment, it fell below the normal range, indicating mild bone marrow suppression.
2. Hb：Hemoglobin levels dropped to 8.7 g/dL prior to the fourth treatment, necessitating close monitoring for anemia.
3. PLT：Platelet counts showed minor fluctuations during the treatment period but remained within the normal range.
4. Cre：Creatinine levels remained stable between 1.0 and 1.4 mg/dL, indicating good renal function.
5. T-Bil：Total bilirubin levels stayed within the normal range throughout the treatment.
6. Alb：Albumin levels slightly declined over the course of treatment, reaching 3.6 g/dL before the fourth session.
7. AST, ALT：Liver function, as reflected by AST and ALT levels, remained within the normal range.

某區域教學醫院肽受體放射性核種治療 (PRRT) 之案例報告

張婉柔　柯冠吟

國立臺灣大學醫學院附設醫院癌醫中心分院 核子醫學部

中文摘要

在神經內分泌腫瘤 (Neuroendocrine tumors，NETs) 的治療領域中，肽受體放射性核種治療 (Peptide Receptor Radionuclide Therapy，PRRT) 作爲一種新興的靶向治療方法，近年來受到了廣泛關注。PRRT 利用了大多數 NETs 細胞表面過表達生長抑素受體 (somatostatin receptors，SSTRs) 的特性，通過將放射性核種鎦 -177 與生長抑素類似物結合，實現對腫瘤細胞的精準標靶治療。這種治療方式不僅能夠有效地將放射性藥物遞送到腫瘤部位，還能最大程度地減少對周圍正常組織的損害，從而提高治療效果並降低副作用。本研究目的旨在報導於本院執行 PRRT 治療的個案，於治療後使用單光子電腦斷層掃描 / 電腦斷層 (Single Photon Emission Computed Tomography, SPECT/CT) 掃描，協助評估治療成效及其影像學變化。

關鍵詞：肽受體放射性核種治療，鎦 -177，單光子電腦斷層掃描 / 電腦斷層

核醫技學誌 2024;21:21-26

接受日期：2024 年 12 月 2 日
通訊作者：張婉柔
聯絡地址：臺北市大安區基隆路三段 155 巷 57 號 B1F 核子醫學部
電話：02-23220322#237954
電子郵件：A01142@ntucc.gov.tw

利用 ^{18}F-FDG 正子電腦斷層造影掃描區分下咽癌和食道癌之影像討論—兩案例報告

黃琪雯 [1,2]　翁瑞鴻 [2]

[1] 中山醫學大學 醫學研究所
[2] 中山醫學大學附設醫院 核子醫學科

摘要

本次病例報告討論兩位 64 歲男性患者利用 ^{18}F-FDG 正子電腦斷層造影 (PET/CT) 掃描檢查以進行癌症分期並訂定治療方針。案例一經胃鏡併切片檢查檢查發現爲食道癌，但 18F-FDG 正子電腦斷層造影 (PET/CT) 掃描影像顯示下咽侵犯範圍更大，故重新判定爲下咽癌；案例二經病理切片證實爲下咽癌，利用 ^{18}F-FDG 正子電腦斷層造影 (PET/CT) 掃描進行治療前分期，發現腫瘤範圍從下咽至食道，且有頸部淋巴結轉移，故由影像判定爲下咽癌，患者得以接受積極的治療規劃。下咽癌和食道癌屬於不同的疾病類型，不僅分期系統不同，其判定期別更影響到後續可接受之治療方法的選擇，且預後和癌症登記亦不相同。同一腫瘤同時侵犯兩器官時，^{18}F-FDG 正子電腦斷層造影 (PET/CT) 掃描能正確鑑別原發部位，有助正確的臨床決策。

關鍵詞：下咽癌，食道癌，正子電腦斷層造影掃描

核醫技學誌 2024;21:27-32

前言

如何決定癌症的治療方式，需依據腫瘤位置、癌症分期、是否爲侷限性或已轉移，後續的治療方針亦有所不同，而許多癌症發生初期，其生理代謝活動變化會發生在解剖變化之前，此時可顯示細胞代謝變化的正子電腦斷層造影掃描就可提供相當大的助力。

正子電腦斷層造影掃描是顯示藥物在體內新陳代謝之情況，若有代謝活動異常之處即可呈現在影像上，是一種功能性影像 (functional imaging) 且爲非侵入性 (non-invasive) 的診斷工具。現今可搭配正子電腦斷層造影掃描用以偵測腫瘤變化使用的放射藥物有許多種類，但目前最常利用腫瘤細胞具有葡萄糖代謝增強的特點，將與葡萄糖結構類似的 ^{18}F-FDG 替代模擬進入細胞，當腫瘤細胞血流增加時，經血液送至腫瘤組織的 ^{18}F-FDG 也隨之增加，用以觀察腫瘤細胞攝取額外葡萄糖的現象做爲癌症診斷的工具。利用此特性，使用 ^{18}F-FDG 進行正子電腦斷層造影掃描提早診斷腫瘤細胞或組織代謝異常是極具優勢的，而且已經廣泛應用在評估多種癌症分期、術前病灶定位、後續治療效果評估，以及偵測癌症復發情況等。

目前國內全民健保給付正子電腦斷層造影掃描在確診爲癌症的適應症爲：乳癌、淋巴癌、大腸癌、直腸癌、食道癌、頭頸癌 (不含腦瘤)、原發性肺癌、黑色素癌、甲狀腺癌及子宮頸癌。[2]

病例報告

利用 ^{18}F-FDG 進行正子電腦斷層造影掃描，腫瘤細胞因耗能較高，在體內消耗葡萄糖的速度會較正常組織細胞快，當放射藥物 ^{18}F-FDG 進入體內會聚積在葡萄糖

接受日期：2024 年 9 月 4 日
通訊作者：翁瑞鴻
聯絡地址：台中市南區建國北路一段 110 號
電話：04-24739595 ext.32002
電子郵件：cshy695@csh.org.tw

代謝異常的區域，而影像上就會顯示異常明亮，明亮處即爲腫瘤位置。

第一位案例因吞嚥困難就醫，此患者經胃鏡檢查發現爲食道癌，進行病理切片檢查證實爲鱗狀細胞癌，爲進行癌症分期並訂定治療方針而進行 ^{18}F-FDG 正子電腦斷層造影掃描。依 ^{18}F-FDG 正子電腦斷層造影掃描影像顯示病灶涉及下咽後壁 (圖一)、環狀軟骨後區 (圖二)、椎前筋膜和上頸食道 (圖三)，異常代謝爲橫向延伸，同時出現多個區域淋巴結轉移。藉由 ^{18}F-FDG 正子電腦斷層造影掃描影像上可判別下咽部腫瘤範圍明顯大於食道部位，故判定原發爲下咽癌，併侵犯食道。後續進行咽喉顯微直視鏡檢查亦確診爲下咽癌。

第二位案例因喉痛就診，病理切片檢查確診爲下咽癌，需藉由 ^{18}F-FDG 正子電腦斷層造影掃描進行癌症分期。^{18}F-FDG 正子電腦斷層造影掃描影像顯示病灶侵犯環狀軟骨後區 (圖四)、椎前筋膜和頸部食道 (圖五)，異常代謝爲縱向延伸，且右側頸部有數個代謝異常的淋巴結 (圖六)，顯示淋巴結轉移，下咽部位腫瘤與食道部分腫瘤大小幾乎相同。若判定爲食道癌，則 M 分期爲 M1；若判定爲下咽癌，則 M 分期爲 M0，則尚有非姑息治療的選擇，故 ^{18}F-FDG 正子電腦斷層造影掃描判定原發爲下咽癌，併侵犯食道。

結論

下咽癌在頭頸部癌症中位居第三，僅次於口腔癌和鼻咽癌。下咽癌多與抽菸、喝酒、嚼食檳榔有關，這些危險因子也容易誘發其他頭頸部腫瘤和食道腫瘤，所以下咽癌常合併上述癌症一起或先後發生。下咽位於口腔和食道的交接處，下咽部位可細分爲梨狀竇、下咽後壁和環狀軟骨後區三個構造組成。下咽癌初期症狀不明顯，常見有耳朵痛、咽喉疼痛及咽喉有異物感，但這些症狀容易和耳鼻喉科疾病，如上呼道感染、慢性咽喉炎等相似，因而極易產生混淆，隨著腫瘤逐漸變大，患者會有頸部腫塊、吞嚥困難、聲音沙啞、體重減輕等症狀，但因多爲咽喉深處，目視檢查無法及時發現，常需內視鏡檢查才能診斷，因此下咽癌確診時，多爲晚期且已轉移至頸部淋巴結。

另一方面，食道癌早期症狀不明顯，晚期症狀則有吞嚥困難，常感覺有食物附著在咽喉或胸部、咳嗽或聲音沙啞等，待發生時亦多爲時已晚且已有淋巴結轉移。下咽和食道兩者生理位置相近，最常見的癌細胞型態亦皆爲鱗狀細胞癌，同時被腫瘤侵犯臨床上亦不罕見。本次案例一的患者即是被認定爲食道癌，因而進一步接受 ^{18}F-FDG 正子電腦斷層造影掃描，進行癌症治療前分期。由影像上顯示發現腫瘤病灶大多位於下咽部位，下咽部分腫瘤比食道部分腫瘤大，因而判定此患者原發爲下咽癌，併侵犯食道。案例二的患者則爲已確診爲下咽癌，^{18}F-FDG 正子電腦斷層造影掃描顯示腫瘤亦侵犯食道；腫瘤侵犯下咽部分與食道部分大小幾乎相同，加上頸部有多個淋巴結轉移。若判定爲食道癌，則淋巴結轉移將會被定義爲遠端轉移 (M1)，只能選擇姑息治療；但若判定爲下咽癌患者，則 M 分期爲無遠端轉移 (M0)，患者尚有非姑息治療的選擇，故 ^{18}F-FDG 正子電腦斷層造影掃描判定原發爲下咽癌，併侵犯食道。

下咽和食道分屬於呼吸道與消化道；下咽癌和食道癌亦分屬於不同的癌症分類，兩者不僅分期系統不同，其預後和癌症登記也不相同，需要正確區別。透過此二病例可見，全身 ^{18}F-FDG 正子電腦斷層造影掃描正可發揮此關鍵作用，是故頭頸癌與食道癌同時爲健保給付之癌別，其重要性可見一斑。

參考文獻

1. 曾凱元 (2006)。核醫正子攝影於癌症之偵測。台灣醫學雜誌，10(2)，224-233。
2. 李將瑄 (2017)。癌症檢查的新武器 -PET 正子放射斷層儀。奇美醫訊，(117)，34-35。

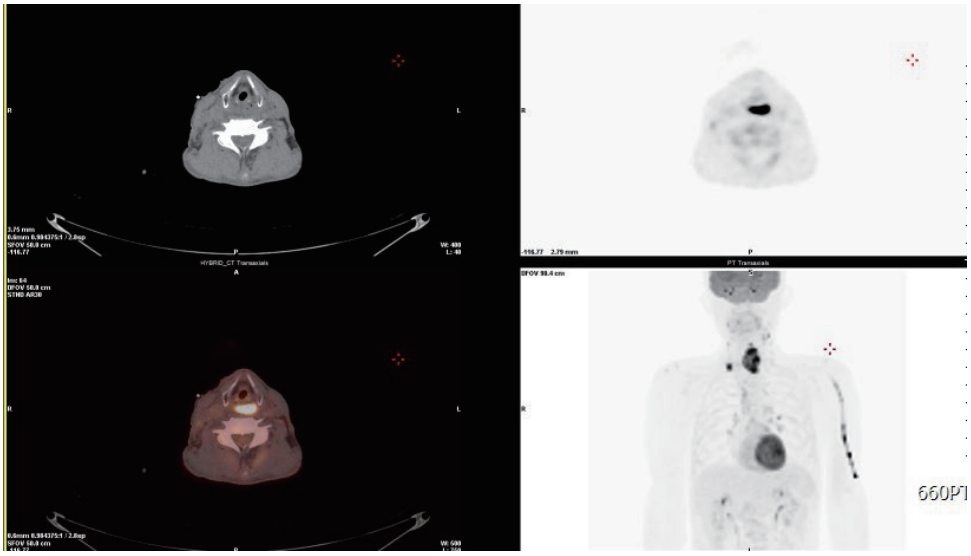

圖一　在正子電腦斷層造影掃描中，影像顯示 ^{18}F-FDG 葡萄糖異常活度吸收涉及下咽後壁。

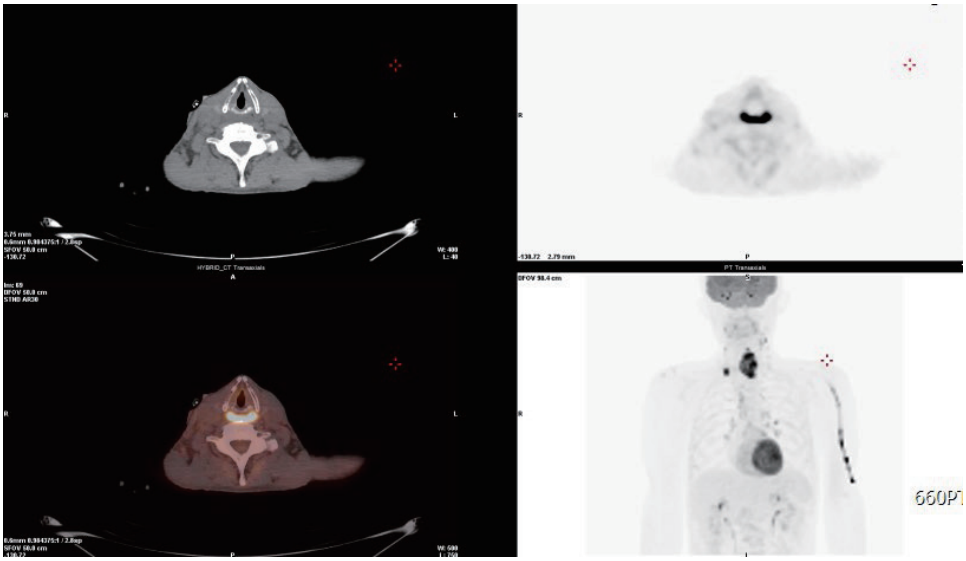

圖二　在正子電腦斷層造影掃描中，影像顯示 ^{18}F-FDG 葡萄糖異常活度吸收涉及環狀軟骨後區域。

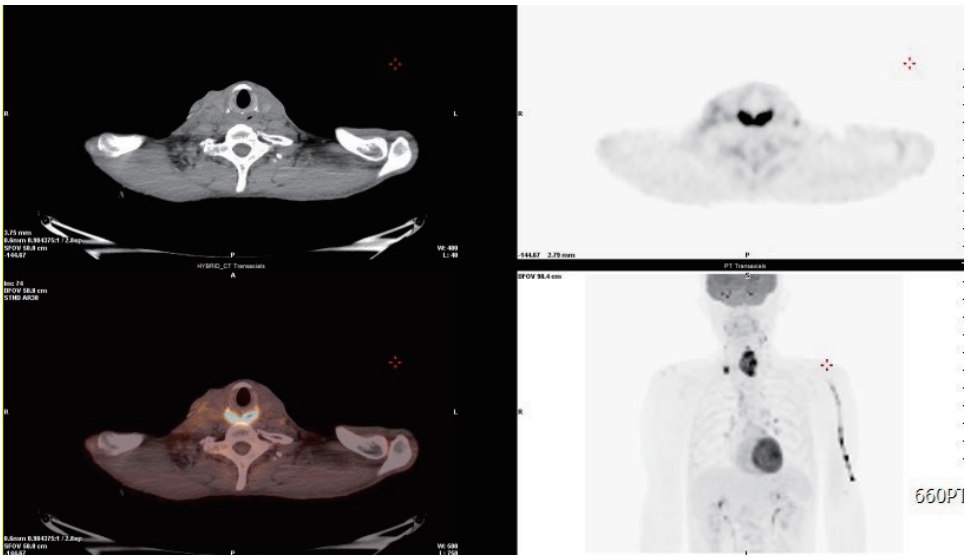

圖三　在正子電腦斷層造影掃描中，影像顯示 ^{18}F-FDG 葡萄糖異常活度吸收涉及上頸食道。

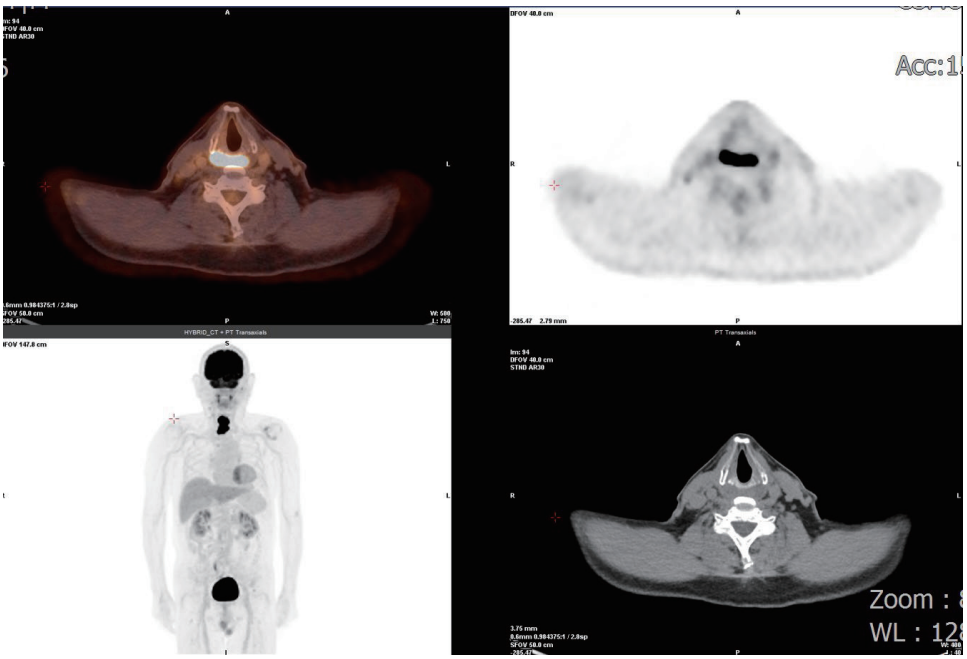

圖四　在正子電腦斷層造影掃描中，影像顯示 ^{18}F-FDG 葡萄糖異常活度吸收涉及環狀軟骨後區域。

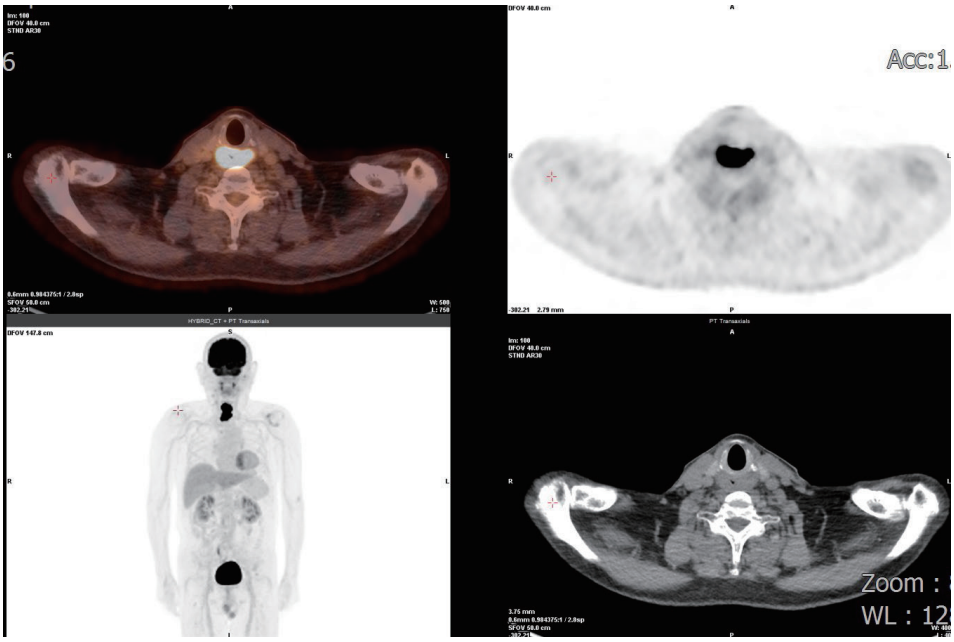

圖五　在正子電腦斷層造影掃描中，影像顯示 ^{18}F-FDG 葡萄糖異常活度吸收涉及頸部食道。

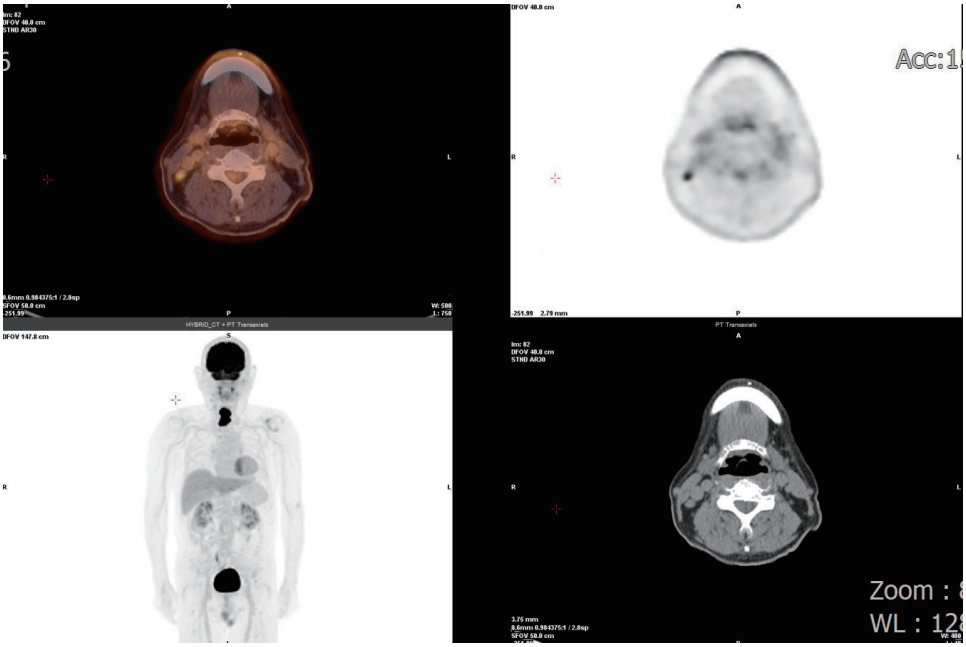

圖六　在正子電腦斷層造影掃描中，影像顯示右側頸部有數個 ^{18}F-FDG 葡萄糖異常活度吸收的淋巴結。

To differentiate hypopharyngeal cancer from cervical esophageal cancer does matter on ^{18}F-FDG PET/CT scan- Two Case Reports

Chi-Wen Huang[1,2], Jui-Hung Weng[2]

[1]*Institute of Medicine, Chung Shan Medical University*
[2]*Department of Nuclear Medicine, Chung Shan Medical University Hospital, Taichung, Taiwan*

Abstract

To performed ^{18}F-FDG positron emission tomography-computed tomography (PET/CT) scan in two 64-year-old males for pre-treatment staging and treatment policy. In case 1, esophageal cancer was impressed by gastroscopy and therefore biopsy was taken. Squamous cell carcinoma was later proven pathologically. The diagnosis was confirmed by endoscopic examination. In case 2 was confirmed to be hypopharyngeal carcinoma by pathological section. The tumor ranged from hypopharynx to esophagus, and there was cervical lymph node metastasis, which was judged to be hypopharyngeal carcinoma by imaging. Hypopharyngeal cancer and cervical esophageal cancer belong to different disease entities. Not only staging systems but also prognosis and cancer registry differ. The staging has a greater impact on the choice of subsequent acceptable treatments. Correct differentiation when interpreting FDG PET/CT scan for such entities is warranted.

Keywords: Hypopharyngeal cancer, esophageal cancer, PET/CT

J Nucl Med Tech 2024;21:27-32

Received 2024/9/4
Corresponding author: Jui-Hung Weng
Address: 402 No. 110, Section 1, Jianguo North Road, Taichung City
Tel: 04-24739595 ext.32002
E-mail: cshy695@csh.org.tw

腎軸旋轉不良導致 FDG 蓄積在輸尿管一案例報告

吳麗君[1]　顏玉安[1]　李將瑄[1,2*]

[1] 奇美醫療財團法人奇美醫院 核醫科
[2] 高雄醫學大學 醫學系

摘要

腎軸旋轉不良 (Malrotation of the Renal Axis) 是罕見的，正常生理腎臟位置爲腎盂朝向內側，腎盞朝向外側，而腎軸旋轉不良可以是任何方向。在 CT、超音波、MRI、核醫 DMSA 及 DTPA 都有文獻報告，但是在正子影像未曾有相關報告，特此提出。

我們報告一例 52 歲鼻咽癌 (nasopharyngeal cancer) 男性，在執行眞正全身 (Real Whole-body) (從頭到腳，包括手和腳) FDG PET/CT(fluorodeoxyglucose Positron emission tomography/computed tomography) 時，意外發現在左腎前外側處有線段 FDG 攝取，單就 PET/CT 會判讀爲腸道分泌，但合併 PET/CT 之 CT 解剖位置判讀爲腎軸旋轉不良，腎盂向左前外側 (left anterolateral)，可能是腎軸旋轉不良導致 FDG 蓄積在輸尿管，爲進一步證實，執行局部延遲像 (delayed imaging) 及進一步局部延遲照影像 (further delayed imaging)，照相前讓病人喝水，走動 20 分鐘，結果減少此處 FDG 攝取。因病情需求，追蹤一年後執行 PET，FDG 無顯著變化，臨床上亦認爲無輸尿管的病灶或轉移，判定此爲腎軸旋轉不良導致 FDG 蓄積在輸尿管。

關鍵詞：FDG、腎旋轉不良、正子

核醫技學誌 2024;21:33-37

接受日期：2024 年 11 月 7 日
通訊作者：李將瑄
單位：奇美醫療財團法人奇美醫院
地址：71004 台南市永康區中華路 901 號
電話：06-2812811-53575；電子郵件：chlee4@ms45.hinet.net

前言

因爲 FDG 從腎臟的生理性排泄會掩蓋輸尿管的病灶，所以輸尿管的病灶在去氧氟化葡萄糖正子放射斷層 / 電腦斷層 (fluorodeoxyglucose Positron emission tomography/computed tomography，FDG PET/CT) 應用會受到限制。腎軸旋轉不良 (Malrotation of the Renal Axis) 是罕見的，在 939 例屍檢中有 1 例發現腎軸旋轉不良，造成原因通常是先天性的。正常生理腎臟位置爲腎盂朝向內側，腎盞朝向外側，而腎軸旋轉不良可以是任何方向，腎盂的方向可以是向前、向後和向外側。在 CT、超音波、MRI、核醫 DMSA 及 DTPA 都有文獻報告 [1-4]，但是在正子影像未曾有相關報告，特此提出。

我們報告一例 52 歲鼻咽癌 (nasopharyngeal cancer) 男性，在執行眞正全身 (Real Whole-body) (從頭到腳，包括手和腳)FDG PET/CT 及局部延遲相 (delayed imaging)，意外發現在左腎前外側 (left anterolateral) 處有線段 FDG 攝取，可能是腎軸旋轉不良導致 FDG 蓄積在輸尿管，執行進一步局部延遲照影像 (further delayed imaging)，結果減少此處 FDG 攝取。因病情需求，追蹤一年後執行正子影像，同一處 FDG 沒有顯著變化，臨床上亦認爲無輸尿管的病灶或轉移，判定腎軸旋轉不良導致 FDG 蓄積在輸尿管。

病例報告

一位 52 歲男性鼻咽癌病人，經化療電療後，因懷疑復發故安排 PET。使用 GE Discovery IQ PET/CT (5 環)，並搭配 Asir 低劑量 CT 及 Xeleris 影像重組軟體 (version3.1)[5-6]。PET 檢查前除白開水以外禁食 6 小時，注射 FDG 前先飲水 300-500ml，檢查前血糖 104 mg/dl，於左手靜脈注射 10 mCi FDG 後，滴入 100ml 生理食鹽水，在密閉昏暗房間內休息 60 分鐘後，飲水 300-500ml 及解尿後，執行全身眞正初期影像 (掃描從頭掃至腳，

含手和腳)，意外發現在左腎前外側處有線段 FDG 攝取 (maximum standardized uptake value，SUVmax 35.2)(圖 1A)，單就 PET/CT 判讀爲腸道分泌，但合併 PET/CT 之 CT 解剖位置 (圖 1E) 判讀爲腎軸旋轉不良，腎盂向左前外側，可能是腎軸旋轉不良導致 FDG 蓄積在輸尿管。

爲進一步證實，執行局部延遲像 (delayed imaging)，掃描前讓病人喝水 300-500ml、飲食並走動 20 分鐘及解尿，預期將促使在腎軸旋轉不良的輸尿管累積的 FDG 流動，將其 FDG 排至膀胱，在注射後 110 分鐘後，從肩膀掃描至骨盆底，結果左輸尿管仍有 FDG 蓄積，但 FDG 攝取顯著減少 (SUVmax 8.0)(圖 1B)。

因左輸尿管仍有蓄積不能確定病灶，爲進一步肯定，執行進一步局部延遲像 (further delayed imaging)，掃描前再讓病人喝水 300-500ml、飲食、走動 20 分鐘及解尿，在注射後 150 分鐘後，從肝臟掃描至骨盆底，結果左輸尿管 FDG 蓄積顯著減少 (SUV max 4.1)(圖 1C)。

合併 PET/CT 之 CT 解剖位置、延遲相及進一步延遲相得知爲本案例爲左腎軸旋轉不良，腎盂面向左前外側，經追蹤一年後執行 PET，FDG 無顯著變化，臨床上亦認爲無輸尿管的病灶或轉移，判定此爲腎軸旋轉不良導致 FDG 蓄積在輸尿管。

討論

原始胚胎腎臟長在骨盆中，腎盂朝向腹側，妊娠 6-9 週時腎臟逐漸上升到腎窩中的成年位置，在上升過程中，腎臟向腹內側旋轉 90 度，使腎盂面向內側。文獻報告腎軸旋轉不良是罕見的 [3]，腎臟旋轉異常通常在水平面（圍繞垂直軸），包括旋轉不足（腎盂面向腹側、側面或背面）、過度旋轉或反向旋轉（腎盂橫向）。旋轉方向一般爲水平旋轉，也有垂直旋轉 [4]。

在本案例經 CT 的影像得知爲腎軸旋轉不良，是屬於依水平面向左外旋轉 135 度，腎盂面向左前外側，其供應血管及輸尿管位置也是朝左前外旋轉，非一般正常位置，故容易蓄積尿液。

輸尿管轉移癌的發生率爲 0.37%[7]，FDG PET 對輸尿管的病灶是可以偵測的 [8-9]，已知輸尿管的病灶在 FDG PET/CT 應用受到限制，是因爲 FDG 會從輸尿管的生理性排泄，可能遮住輸尿管的病灶。

在本案例因輸尿管有 FDG 蓄積爲避免病灶被遮住，所以我們利用局部延遲像及進一步局部延遲像，讓病人飲食、喝水，走動 20 分鐘及解尿，促使在腎軸旋轉不良的輸尿管累積的 FDG 流動，減少 FDG 攝取，經追蹤一年後執行 PET，FDG 無顯著變化，臨床上亦認爲無輸尿管的病灶或轉移，判定此爲腎軸旋轉不良導致 FDG 蓄積在輸尿管。

結論

當在 PET 上有顯示腎臟附近有線狀 FDG 蓄積，先以 PET/CT 之 CT 解剖位置確定是否屬於腎軸旋轉不良的病人，可能是輸尿管蓄積，必要時執行延遲像或第二次局部延遲像，掃描前請病人喝水，走動 20 分鐘及解尿，促使累積在輸尿管 FDG 流動並排至膀胱，使蓄積處減少 FDG 攝取，判定此爲腎軸旋轉不良導致 FDG 蓄積在輸尿管，可有效排除輸尿管的病灶。

參考文獻

1. Divjak, N., et al., *Hydronephrosis caused by kidney malrotation*. Urol Case Rep, 2021. 36: p. 101564.
2. Lim, T.J., et al., *Renal cell carcinoma in a right malrotated kidney*. Korean J Urol, 2011. 52(11): p. 792-4.
3. Tsai, H.Y., et al., *Sagittally malrotated kidney: a case series of two patients*. Surg Radiol Anat, 2015. 37(5): p. 551-3.
4. Ueno, K., et al., *False-positive technetium-99m DMSA renal imaging in two cases of malrotated kidney*. Clin Nucl Med, 1985. 10(7): p. 504-6.
5. Boellaard, R., et al., *FDG PET/CT: EANM procedure guidelines for tumour imaging: version 2.0*. Eur J Nucl Med Mol Imaging, 2015. 42(2): p. 328-54.
6. Yen, Y.A., et al., *Does Routine Triple-Time-Point FDG PET/CT Imaging Improve the Detection of Liver Metastases?* Diagnostics (Basel), 2020. 10(9).
7. Arvind, N.K., et al., *Ureteral metastasis as the presenting manifestation of pancreatic carcinoma*. Rev Urol, 2013. 15(3): p. 124-30.
8. Cervino, A.R., et al., *The role of PET/CT in the evaluation of patients with urothelial cancer: a systematic review and meta-analysis*. Clinical and Translational Imaging, 2018. 6(2): p. 77-89.
9. Zattoni, F., et al., *(18)F-FDG PET/CT and Urothelial Carcinoma: Impact on Management and Prognosis-A Multicenter Retrospective Study*. Cancers (Basel), 2019. 11(5).

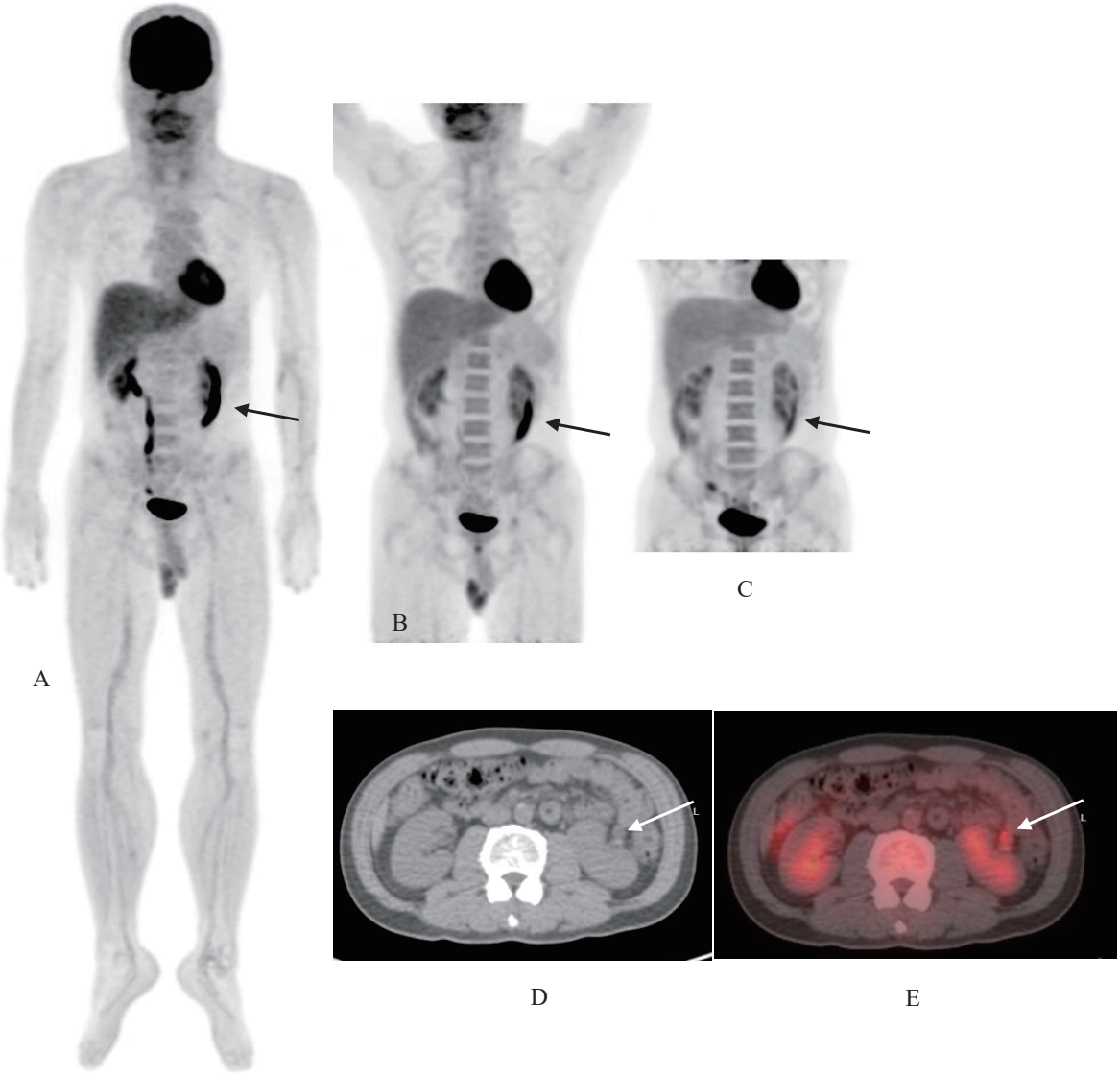

Fig 1. 一位 52 歲鼻咽癌 (nasopharyngeal cancer) 男性病人因懷疑復發故安排 PET 影像，在初期影像 (A 圖) 左腎前外側有線段 FDG 攝取 (箭頭)，延遲像 (B 圖) 顯示此處 FDG 攝取減少並且 SUVmax 值減少 (35.2→8.0)，進一步局部延遲像 (C 圖) 顯示此處 FDG 攝取減少 (SUV max 4.1)，FDG 明顯減少。在橫切 CT 及 PET/CT Fused (D 圖和 E 圖) 影像顯示左腎盂面向左外側，其左輸尿管位置也是朝左前外旋轉約 135 度。

Fig 2. 同一位病人在一年後的 PET，在初期影像 (A 圖) 及延遲像 (B 圖) 的左腎 (箭頭)FDG 攝取減少並且 SUVmax 值減少 (18.93→4.78)，病情也沒有轉移到此部位，臨床醫師亦認爲無腎臟的病灶或轉移，判定爲腎臟旋轉不良導致 FDG 蓄積在輸尿管。

Malrotation of the renal axis leading to ureteral accumulation in positron emission imaging: a case report.

Li-Chun Wu[1], Yu-An Yen[1], Chiang-Hsuan Lee[1,2*]

[1]*Department of nuclear medicine, Chi Mei Medical Center, Yongkang, Tainan, Taiwan*
[2]*School of Medicine, Kaohsiung Medical University*

Abstract

Malrotation of the Renal Axis is rare, with the normal physiological position of the kidneys being the renal pelvis facing medially and the calyces facing laterally, whereas malrotation can occur in any direction. There are reports in literature regarding this condition in CT, ultrasound, MRI, and nuclear medicine DMSA and DTPA, but no related reports in positron emission imaging have been documented, hence this presentation.

We report a case of a 52-year-old male with nasopharyngeal cancer who underwent a Real Whole-body FDG PET/CT scan (from head to toe, including hands and feet). During the scan, an incidental finding of segmental FDG uptake was observed in the anterolateral aspect of the left kidney. On PET/CT, this would typically be interpreted as intestinal secretion, but when combined with the CT anatomical interpretation, it was identified as malrotation of the renal axis, with the renal pelvis directed towards the left anterolateral side. This malrotation likely caused the accumulation of FDG in the ureter. To further confirm this, we conducted delayed imaging and additional delayed imaging after having the patient drink water and walk for 20 minutes prior to the imaging. This resulted in a decrease in FDG uptake in that area. After one year of follow-up, the FDG uptake remained similar, and clinically, it was considered that there were no lesions or metastasis in the ureter, concluding that the accumulation of FDG in the ureter was due to malrotation of the renal axis.

Keywords: Malrotation of the Renal Axis, PET/CT, FDG

J Nucl Med Tech 2024;21:33-37

Received 2024/11/7
Corresponding author: Chiang-Hsuan Lee
Department od nuclear medicine, Chi Mei Medical Center
Address: No.901, Zhonghua Rd., Yongkang Dist., Tainan City 710, Taiwan
Tel: 06-2812811-53575; E-mail: chlee4@ms45.hinet.net

I-131 掃描與 FDG PET/CT 掃描對甲狀腺癌復發轉移之影像探討

朱秀蘭[1]　游慧貞[2]　劉芝庭[3*]

[1] 高雄醫學大學附設中和紀念醫院 核子醫學部
[2] 高雄醫學大學附設中和紀念醫院 影像醫學部
[3] 中國醫藥大學新竹附設醫院 核子醫學科

摘要

本次病例報告討論一位甲狀腺癌男性患者，後續於健檢的低劑量電腦斷層影像中發現復發轉移至肺部，因此進行放射性碘 -131 治療，但其碘 -131 掃描結果除在腸胃道處有放射活性聚集現象疑爲糞便之外，並未發現有其他異常轉移。故再接受正子斷層掃描檢查，影像中發現薦骨處有異常放射吸收，與之前碘 -131 掃描影像比對後，發現其相對位置亦有異常活性吸收，代表此前影像中腸胃道處放射性聚集現象並非是糞便，而是甲狀腺癌轉移至薦骨處。

關鍵詞：甲狀腺癌，碘 -131 掃描，正子斷層掃描

核醫技學誌 2024;21:39-42

前言

在人體中，甲狀腺組織是唯一可以攝取碘的器官，可經由碘分子通道 (NaI symporter) 將碘攝入甲狀腺細胞，合成甲狀腺素以調節人體代謝功能。當甲狀腺發生異常時，患者大多沒有感覺，但即使被診斷爲甲狀腺癌，其中 98% 甲狀腺癌爲分化良好，若能早期接受完整治療及定期追蹤，五年存活率大多有 87% 以上，但一些病人會發生再發性或甚至死亡 [1]。甲狀腺癌的主要治療包括：(1) 手術治療：分爲甲狀腺單葉部分切除或全葉切除，爲最常見且有效的治療方式。(2) 放射性碘 -131 治療 : 爲術後輔助治療，用於治療剩餘的甲狀腺癌細胞。(3) 甲狀腺激素療法 : 服用甲狀腺激素 (TSH) 抑制甲狀腺癌生長。(4) 標靶藥物治療 (5) 放射線治療 (6) 化學藥物治療 [2、3、4]。

目前公認治療分化型甲狀腺癌的最佳治療方式爲手術切除腫瘤加上放射碘治療，其中 I-131 之適應症包括：無法開刀之原發性腫瘤、頸部開刀後殘餘之腫瘤、遠部轉移、頸部與縱膈之淋巴腺轉移、肺部轉移及再發甲狀腺癌 [5]。I-131 爲碘的一種放射性同位素，同時釋放 γ 及 β 兩種放射線，經由碘分子通道而被甲狀腺細胞攝取。其中，γ 放射線穿透力較強，可以從體外偵測甲狀腺細胞攝取 I-131 的情況，以瞭解甲狀腺的功能及診斷病灶轉移的狀況。

病例報告

一位 63 歲男性患者，於 2015 年診斷出甲狀腺癌並於同年 2 月手術切除，後於 2016 年 3 月及 2017 年 7 月進行放射性碘 -131 治療。在 2022 年 7 月公司健檢的低劑量電腦斷層影像中發現復發轉移至肺部，再次於 2023 年 3 月進行放射性碘 -131 治療。此次碘 -131 影像檢查結果，除在腸胃道處有放射活性聚集現象疑爲糞便之外 (圖一及圖二)，並未發現有其他異常轉移，故建議病患透過正子斷層攝影檢查進一步確認是否爲放射碘難治分化型甲狀腺癌。

患者於 2023 年 4 月執行正子檢查，在檢查影像中發現薦骨處有異常放射吸收 (圖三)，與之前碘 -131 掃描影像比對後，發現其相對位置亦有碘 -131 異常活性吸收，代表此前影像中腸胃道處放射性聚集現象並非是糞便，而是甲狀腺癌轉移至薦骨處。

接受日期：2024 年 12 月 9 日
通訊作者：劉芝庭
地址：新竹縣竹北市興隆路一段 199 號
電話：03-5580558 轉 1477
電子郵件：sindysmile@yahoo.com.tw

結論

碘 -131 掃瞄檢查時，因身體前後器官重疊，在平面影像上不好區分病灶位置，而大多於在甲狀腺處進一步執行 SPECT/CT 掃描，提供解剖定位更精確之融合影像 [6]。但在腸胃道部位即使有異常放射性活性吸收，容易被認爲是碘 -131 藥物正常代謝而被誤判。因此在平面掃描後，若在身體其他部位發現有放射活性聚集現象，仍需加以執行 SPECT/CT 掃描來評估是否爲轉移，以此交叉對照協助確認患者實際狀況及找出轉移之位置，期能提高判讀正確性及提供臨床更佳診斷價值。

參考文獻

1. 廖廣義 (2004)。甲狀腺癌之新進展。台灣醫學，8(1)，1-9。https://doi.org/10.6320/FJM.2004.8(1).01
2. Schlumberger MJ. Papillary and follicular thyroid carcinoma. N Engl J Med 1998;338:297-306.
3. 洪堯民、黃二榮 (1991)。分化良好甲狀腺癌的手術治療與預後評估。當代醫學，(211)，388-398。https://doi.org/10.29941/MT.199105.0010
4. 劉文川、蕭信昌、張正權 (2000)。分化良好甲狀腺癌的分析研究。The Changhua Journal of Medicine，6(1)，19-23。https://www.airitilibrary.com/Article/Detail?DocID=16801504-200001-6-1-19-23-a
5. Huang, W. S., Lin, Y. S., & Wu, S. Y. (2005). Nuclear Medicine in the Management of Patients with Well-differentiated Thyroid Carcinoma. 核子醫學雜誌, 18(4), 191-193. https://doi.org/10.6332/ANMS.1804.001
6. Hsieh, J. F., Tan, R., Lee, C. H., & Wu, C. S. (2012). A False-Positive Radioiodine-131 Whole-Body Scan in Thyroid Carcinoma Caused by Menstruation Localized on SPECT/CT. 核子醫學雜誌 , 25(2), 89-91. https://doi.org/10.6332/ANMS.2502.008

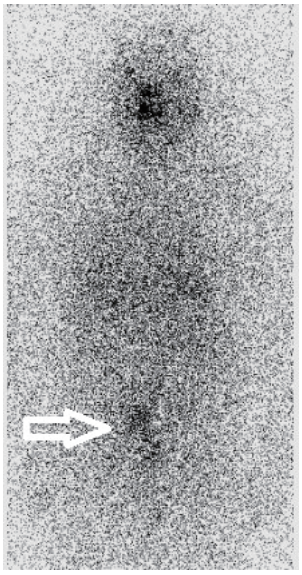

圖一 在 I-131 掃描的正面影像中，發現在腸胃道處有異常的放射性活性聚集。

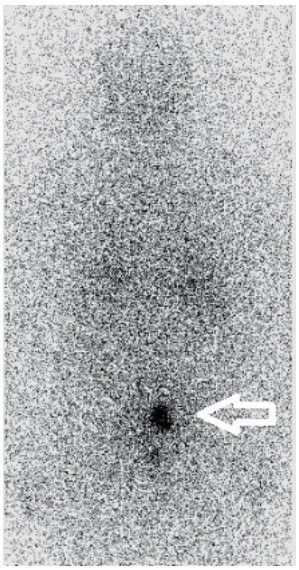

圖二 在 I-131 掃描的背面影像中，發現在腸胃道處有異常的放射性活性聚集。

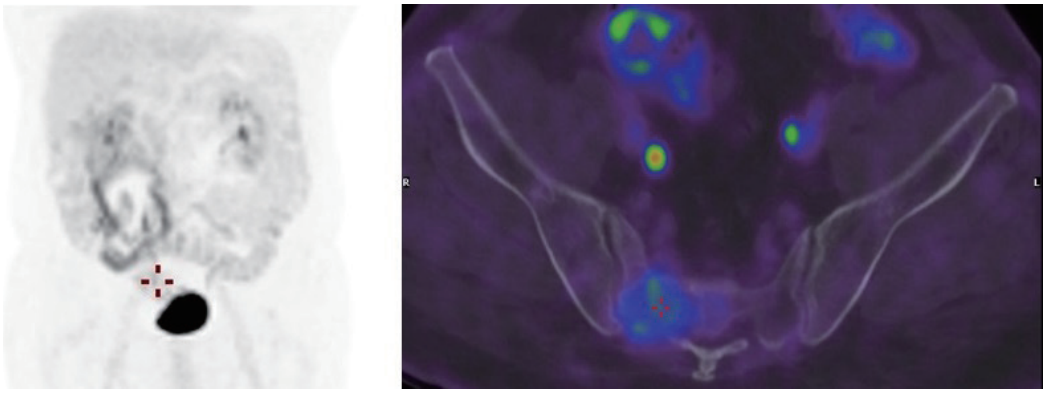

圖三 在正子斷層攝影檢查中，發現薦骨處有異常放射吸收，爲甲狀腺癌轉移至薦骨處。

Role of I-131 Scan and FDG PET/CT Imaging in the Evaluation of Thyroid Cancer Recurrence and Metastasis

Hsiu-Lan Chu[1], Hui-Chen Yu[2], Chih-Ting Liu[3]

[1]*Department of Nuclear Medicine, Kaohsiung Medical University Hospital, Kaohsiung Medical University, Kaohsiung, Taiwan*
[2]*Department of Medical Imaging, Kaohsiung Medical University Hospital, Kaohsiung Medical University, Kaohsiung, Taiwan*
[3]*Department of Nuclear Medicine, China Medical University Hsinchu Hospital, Hsinchu, Taiwan*

Abstract

This case report discusses a male patient with thyroid cancer, who was later found to have distant recurrence in lungs through low-dose CT scan. The patient underwent I-131 therapy for recurrence treatment; however, the I-131 scan revealed no abnormal metastasis except for radioactive accumulation in the gastrointestinal tract, initially suspected to be fecal matter. Subsequently, the patient underwent FDG PET/CT imaging, which identified abnormal uptake in the sacrum. A comparison with the previous I-131 scan revealed that the location of the abnormal uptake corresponded to the previously noted gastrointestinal radioactive accumulation. This finding indicated that the observed activity was not fecal matter but rather a distant recurrence of thyroid cancer in sacrum.

Keywords: Thyroid cancer, I-131 scan, PET/CT

J Nucl Med Tech 2024;21:39-42

Received 2024/12/9
Corresponding author: Chih-Ting Liu
Address:
Tel: 03-5580558#1477
E-mail: sindysmile@yahoo.com.tw

胸椎骨贅導致在 PET 上有 FDG 攝取一案例報告

吳麗君[1]　顏玉安[1]　李將瑄[1,2*]

[1] 奇美醫療財團法人奇美醫院 核醫科
[2] 高雄醫學大學 醫學系

摘要

脊椎骨贅在脊椎病中極爲常見。到 50 歲時，大約 80% 的男性和 60% 的女性會出現骨贅 (osteophytes)。骨贅或稱骨刺 (bone spurs）是一種生長在脊椎或關節周圍骨骼上的骨塊。當關節或骨骼因關節炎受損時就會形成它們，但並非總是會造成問題。

已知在正子放射斷層 / 電腦斷層 (Positron emission tomography/computed tomography，PET/CT) 的電腦斷層 (computed tomography,CT) 影像上，胸椎的骨贅會在靠近胸椎的肺臟處，因爲壓迫導致常有片狀不透明區 (patchy opacity 或局部間質混濁 (focal interstitial opacity) 會有微弱去氧氟化葡萄糖 (fluorodeoxyglucose,FDG) 攝取，一般判讀爲良性，起因爲骨贅刺激肺臟組織造成發炎。但我們報告一例，CT 影像上有骨贅，在 PET 影像上，在靠近右側胸椎的肺臟的初期掃描影像有 FDG 微弱攝取，延遲掃描影像 FDG 攝取無顯著增加，追蹤半年 PET，無顯著變化，判讀爲良性，故特此提出報告。

關鍵詞：胸椎，骨贅，PET/CT，FDG

核醫技學誌 2024;21:43-46

前言

脊椎骨贅在脊椎病中極爲常見。到 50 歲時，大約 80% 的男性和 60% 的女性會出現骨贅 (osteophytes)。骨贅或稱骨刺 (bone spurs）是一種生長在脊椎或關節周圍骨骼上的骨塊。當關節或骨骼因關節炎受損時就會形成它們，但並非總是會造成問題。

已知在正子放射斷層 / 電腦斷層 (Positron emission tomography/computed tomography，PET/CT) 的電腦斷層 (computed tomography,CT) 影像上，胸椎的骨贅會在靠近胸椎的肺臟處，因爲壓迫導致常有片狀不透明區 (patchy opacity 或局部間質混濁 (focal interstitial opacity) 會有微弱去氧氟化葡萄糖 (fluorodeoxyglucose,FDG) 攝取，一般判讀爲良性，起因爲骨贅刺激肺臟組織造成發炎 [1]。但我們報告一例，CT 影像上有骨贅，在 PET 影像上，在靠近右側胸椎的肺臟的初期掃描影像有 FDG 微弱攝取，延遲掃描影像 FDG 攝取無顯著增加，追蹤半年 PET，沒有顯著變化，判讀爲良性，故特此提出報告。

病例報告

一位 62 歲男性頭頸部癌 (鱗狀細胞癌) 病人。因懷疑復發，安排 PET/CT 檢查。檢查前禁食 6 小時，檢查前血糖 100 mg/dl，於左手肘靜脈注射 10 mCi FDG 後，以 100ml 生理食鹽水點滴滴入，在密閉昏暗房間內休息 60 分鐘後，執行初期掃描 (initial scan)。注射後 90 分鐘後執行延遲掃描 (delayed scan)，注射後 110-120 分鐘後執行進一步延遲相。使用 GE Discovery IQ PET/CT (5 環)，並搭配 Asir 低劑量 CT 及 Xeleris 影像重組軟體 (version3.1)。[2-3]

結果在鄰近胸椎的 CT 影像上有骨贅，PET 影像看到靠近胸椎的肺臟有局部 FDG 攝取 (SUV max 1.62 vs. 2.03 vs. 2.11) (圖 1A)，半年後的 PET/CT 同一部位 FDG 攝取 (SUV max 1.21 vs. 1.02) (圖 1B)，無顯著變化，因有前次經驗，故只照延遲相，未有進一步延遲相影像，判定此形成骨贅造成片狀不透明區，屬於發炎，排除轉移之僞陽性。

接受日期：2024 年 12 月 23 日
通訊作者：李將瑄
單位：奇美醫療財團法人奇美醫院
地址：71004 台南市永康區中華路 901 號
電話：06-2812811-53575；電子信箱：chlee4@ms45.hinet.net

討論

片狀不透明區有兩種型態爲網狀及線性，研究指出片狀不透明區由骨贅的直接壓迫所引起的，推測是因爲骨贅的刺激，造成肺臟有片狀不透明區及微弱 FDG 攝取。所以當遇到在靠近胸椎的肺臟有片狀不透明區及微弱 FDG 攝取，鄰近胸椎 CT 影像上雖然有骨刺時，應判讀爲良性 [1]。

結論

所以當遇到在靠近胸椎的肺臟有片狀不透明區及微弱 FDG 攝取，CT 影像上有骨贅時，應判讀爲良性。

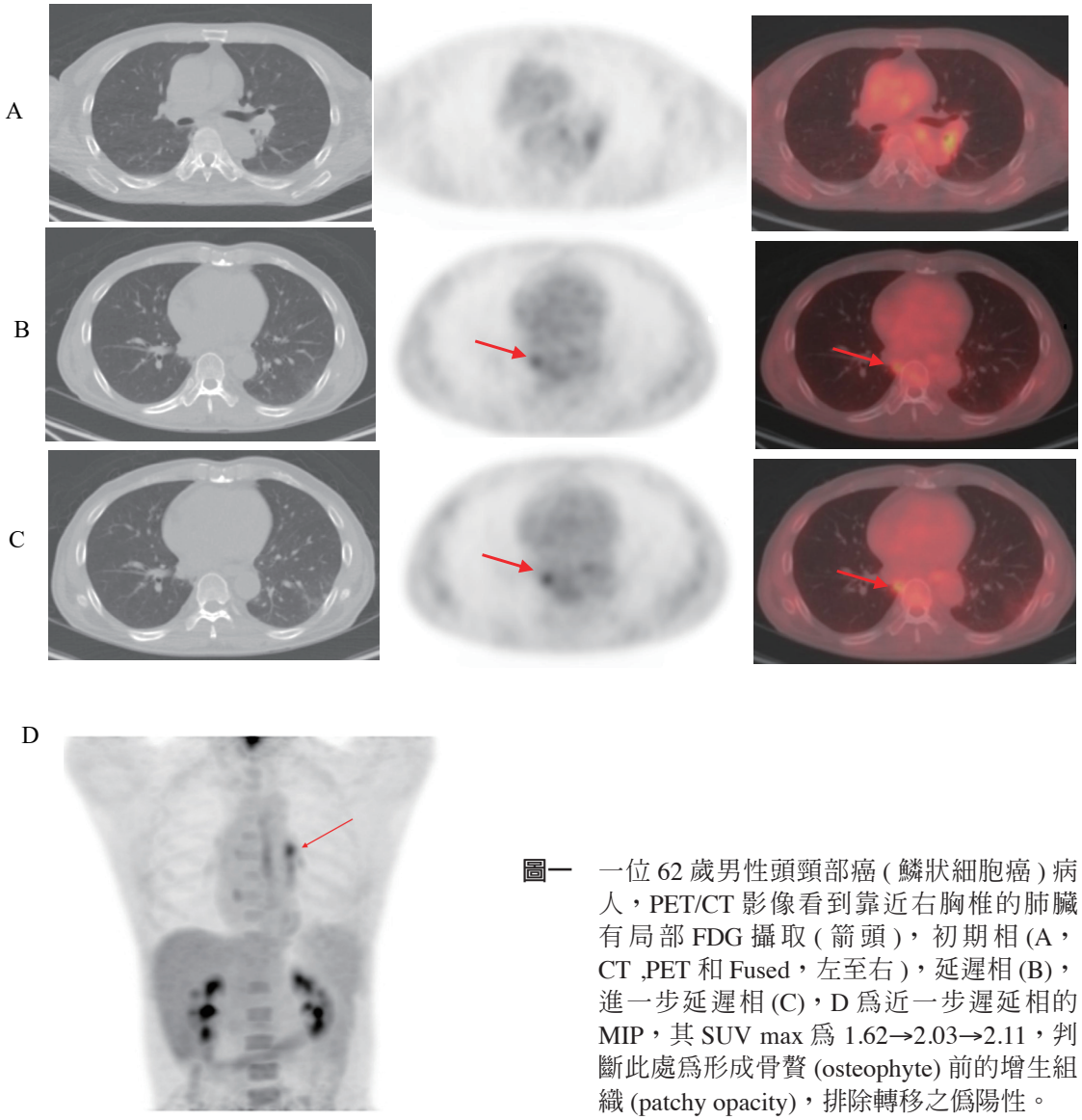

圖一 一位 62 歲男性頭頸部癌 (鱗狀細胞癌) 病人，PET/CT 影像看到靠近右胸椎的肺臟有局部 FDG 攝取 (箭頭)，初期相 (A，CT ,PET 和 Fused，左至右)，延遲相 (B)，進一步延遲相 (C)，D 爲近一步遲延相的 MIP，其 SUV max 爲 1.62→2.03→2.11，判斷此處爲形成骨贅 (osteophyte) 前的增生組織 (patchy opacity)，排除轉移之僞陽性。

參考資料

1. Ulaner, G.A., *Fundamentals of Oncologic PET/CT.* Elsevier ed. 2019. 93.
2. Boellaard, R., et al., *FDG PET/CT: EANM procedure guidelines for tumour imaging: version 2.0.* Eur J Nucl Med Mol Imaging, 2015. 42(2): p. 328-54.
3. Yen, Y.A., et al., *Does Routine Triple-Time-Point FDG PET/CT Imaging Improve the Detection of Liver Metastases?* Diagnostics (Basel), 2020. 10(9).

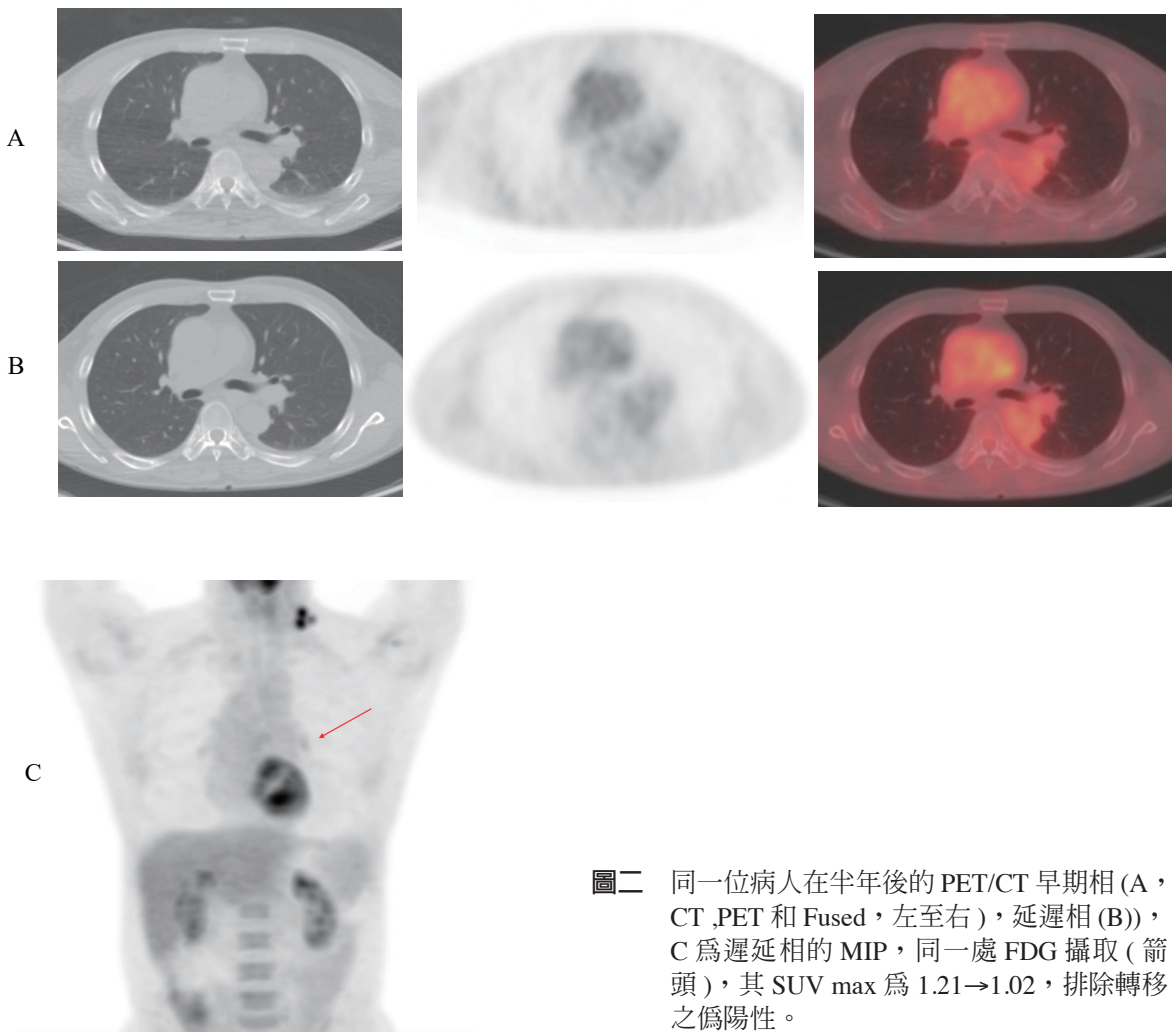

圖二 同一位病人在半年後的 PET/CT 早期相 (A，CT ,PET 和 Fused，左至右)，延遲相 (B))，C 爲遲延相的 MIP，同一處 FDG 攝取 (箭頭)，其 SUV max 爲 1.21→1.02，排除轉移之僞陽性。

Thoracic Osteophytes Leading to FDG Uptake on PET: A Case Report

Li-Chun Wu[1], Yu-An Yen[1], Chiang-Hsuan Lee[1,2*]

[1]*Department of nuclear medicine, Chi Mei Medical Center, Yongkang, Tainan, Taiwan*
[2]*School of Medicine, Kaohsiung Medical University*

Abstract

Bone spurs are extremely common in spinal diseases. By the age of 50, approximately 80% of men and 60% of women will have osteophytes. Bone spurs, also known as osteophytes, are bony growths that develop on the spine or around joints. They form when joints or bones are damaged due to arthritis, but they do not always cause problems.

It is known that on computed tomography (CT) images from positron emission tomography/computed tomography (PET/CT), bone spurs in the thoracic vertebrae can lead to patchy opacities or focal interstitial opacities in the adjacent lung tissue due to compression, which typically shows mild fluorodeoxyglucose (FDG) uptake, generally interpreted as benign, caused by inflammation from bone spur irritation of lung tissue. However, we report a case where CT images showed bone spurs, and in the initial PET scan, there was mild FDG uptake in the lung near the right thoracic vertebra, with no significant increase in FDG uptake in delayed scans. Over three years of follow-up with chest X-rays showed no lung lesions, interpreted as benign, hence this report is presented.

Keywords: Thoracic, Osteophyte, PET/CT, FDG

J Nucl Med Tech 2024;21:43-46

Received 2024/12/23
Corresponding author: Chiang-Hsuan Lee
Department od nuclear medicine, Chi Mei Medical Center
Address: No.901, Zhonghua Rd., Yongkang Dist., Tainan City 710, Taiwan
Tel: 06-2812811-53575; E-mail: chlee4@ms45.hinet.net

建置臺灣醫事放射職類核子醫學領域可信賴專業活動

龔瑞英[1,2,3] 杜高瑩[1,4] 許幼青[1,5] 陳怡勳[1,6] 張婉柔[1,7] 張振榮[3] 蔡世傳[2,3#] 陳惠萍[1,8*]

[1] 中華民國醫事放射師公會全國聯合會
[2] 臺中榮民總醫院 核子醫學科
[3] 中臺科技大學 醫學影像暨放射科學系
[4] 馬偕紀念醫院 核子醫學科
[5] 佛教慈濟醫療財團法人大林慈濟醫院 核子醫學科
[6] 戴德森醫療財團法人嘉義基督教醫院 核子醫學科
[7] 國立臺灣大學醫學院附設醫院癌醫中心分院 核子醫學部
[8] 台東基督教醫院 核子醫學科

摘要

近年來醫學教育邁向以勝任能力爲導向的醫學教育(Competency-Based Medical Education, CBME)，爲了讓勝任能力架構落實應用於日常醫療行爲中，除現有的評核架構外，2020 年中華民國醫事放射師公會全國聯合會 (全聯會) 開始建立全國共識版 EPAs 表單，核子醫學領域於同年度完成「正子電腦斷層造影檢查」及「單光子斷層造影檢查」EPAs 表單。本研究中，全聯會擬透過專家共識新增兩項「核醫藥物與品保」及「同位素治療」EPAs，初步由專家小組撰寫 EPAs 中各項 OPA 及觀察面向，2023 年 3 月進行全國問卷普查，一共取得 60 家核醫單位回覆。2023 年 6 月 10 日全聯會舉行全國共識，邀請全國醫事放射職類核子醫學領域醫學教育專家共 43 名出席，其中包括 (準) 醫學中心代表 18 位、區域醫院代表 23 位、地區醫院代表 2 位。首先由醫學教育專家進行可信賴專業活動介紹與共識教育訓練，接續進入共識建立與 EPAs 建置。本次團隊共識使用「名義團體法」(Nominal Group Technique, NGT) 進行 EPAs 下各任務名稱觀察面向的討論及表決，一共進行 42 項次的團體表決，表決後 18 項次維持原名稱，9 項次修改觀察面向名稱，8 項次合併觀察面向，7 項新增案撤案；接著使用「修正式德菲法」(Modified Delphi Method, MDM) 進行共識程度投票，共識程度分別爲 4.89 及 4.91 分，完成「核醫藥物與品保」及「同位素治療」EPAs 建置。

關鍵詞：勝任能力爲導向的醫學教育，可信賴專業活動，名義團體法，修正式德菲法

核醫技學誌 2024;21:47-60

前言

勝任能力爲導向的醫學教育 (Competency-Based Medical Education, CBME) 的概念在 1970 年代被提出來，最初的定義是在符合當地實際情況，滿足當地需求下，醫療專業人員在一定層級的熟練程度下從事醫療行爲 [1]。相較於傳統單純以訓練期程作爲學習者是否完成訓練，勝任能力爲導向的醫學教育是一種不強調時間爲基礎的訓練、重視學習成果、強調能力、以促進學習者爲中心的教學模組 [2]。

根據 CBME 最初的定義，也爲了讓勝任能力架構能落實於日常醫療行爲中，1999 年美國畢業後醫學教育評鑑委員會 (Accreditation Council for Graduate Medical. Education, ACGME) 與美國醫療專科委員會 (American Board of Medical Specialties, ABMS) 訂定住院醫師需要的六大核心能力，包括：病人照護、醫學知識、執業中學習與改進、人際與溝通技巧、專業素養和制度中執行

接受日期：2024 年 12 月 20 日
* 通訊作者
聯絡人：陳惠萍
地址：台東縣台東市開封街 350 號
電話：089-960888#8172
傳眞：089-341729
電子郵件：a13026@tch.org.tw

共同通訊作者
聯絡人：蔡世傳
地址：臺中市西屯區臺灣大道 4 段 1650 號
電話：(04) 2359-2525 ext.4800
電子郵件：sctsai@vghtc.gov.tw

醫業 [3]，臺灣也引進該制度並依照該架構來評核及訓練住院醫師 [4]。醫事放射師必須培養具備的核心能力概念 (以病人爲中心的醫療、跨領域的團隊合作照護、實證醫學的執行、促進醫療品質、資訊技術利用) 則首度於 2013 年被提出 [5]，台灣醫事放射師全國聯合會 (全聯會) (Taiwan Association of Medical Radiation Technologists, TAMRT) 在 2014 年邀請全國醫事放射專家進行評估共識，建置放射師五大核心能力，包括醫學影像及放射科學知識、醫病關係及團隊溝通能力、病人照護、提升本職技能、專業素養，目前已正式列入醫策會之臨床醫事人員培訓計畫二年期醫事放射師訓練課程指引與醫學影像技放射科學系 (科) 學生臨床實習護照中。

爲了讓 CBME 能夠從概念性的架構，進而落實在平時的臨床教學訓練評估中，許多醫學教育領域的學者及機構提出具體做法，其中最具影響力及說服力的做法，一是美國畢業後醫學教育評鑑委員會 (Accreditation Council for Graduate Medical Education, ACGME) 在 2008 年時所發佈的里程碑計畫 (Milestones Project) [6]，二是荷蘭醫學教育專家 Olle ten Cate 在 2005 年提出的可信任專業活動 (Entrustable Professional Activities, EPAs) [7]。里程碑進行的是學員整體能力進展過程的描述及評估。EPAs 則是評估學員執行臨床任務的整體表現，決定學員是否具備足夠的能力，被信任的執行該項臨床任務 [2]。

EPAs 的架構原先應用於畢業後醫學教育訓練中，後來許多醫學專科設計建構了屬於自身專科的 EPAs [8, 9]，此概念更推展至大學教育以及其他醫療專業領域中 [10]。臺灣急診醫學會自 2011 年開始積極推動 CBME 的在地化，2016 年「台灣急診醫學里程碑計畫第一版」推出後隨即開始著手發展在地化的 EPAs [2]。同年，臺大醫院醫學教育專家楊志偉醫師與臺大醫院放射腫瘤科透過共識建立法建置醫事放射治療領域 EPAs [11]，全聯會全國臨床師資培訓課程自 2017 年開始加入 CBME 相關課程，並帶入可信賴專業活動及里程碑之觀念，逐步向全國臨床教師推廣。2020 年全聯會偕同放射診斷及核子醫學專家，建立放射診斷及核子醫學領域 EPAs，建置過程包含初步撰寫、全國問卷普查、團隊共識，核醫領域於該年度完成「正子電腦斷層造影檢查」及「單光子斷層造影檢查」EPAs[12]。

本研究中，全聯會擬建立「同位素治療」及「核醫藥物與品保」兩項 EPAs 之可觀察執業活動 (Observable Practice Activity, OPA) 與觀察面向，希望透過全國共識方法逐步擴增 CBME 工具。

材料與方法

共識草案撰寫與問卷調查

本研究由全聯會主持，於 2023 年 3 月先邀請核醫實務經驗十年以上專家小組進行草案撰寫，初步將「同位素治療」拆解成 3 個 OPA，包括：治療前準備、執行同位素治療、治療後處置 (表一)；「核醫藥物與品保」也拆解成 3 個 OPA，包括；使用前準備、執行藥物偵測、使用後處置；各 OPA 項目下逐一列出 4-5 項不等的觀察面向 (表二)。草案完成後，全聯會將兩項 EPAs 分別列爲 19 項議案及 16 項議案，隨即以公文方式將議案草案送至全國各核醫科，收集全國初步意見。

觀察面向討論及共識

專家共識於 2023 年 06 月 10 日召開，全聯會邀請全國醫事放射職類核子醫學領域醫學教育專家共 43 名出席，包括 (準) 醫學中心代表 18 位、區域醫院代表 23 位、地區醫院代表 2 位。由臺大醫院醫學教育專家楊志偉醫師進行可信賴專業活動介紹與共識教育訓練，本次團隊共識使用「名義團體法」(Nominal Group Technique, NGT) 進行 EPAs 下各任務名稱觀察面向的討論及表決，所有專家對於該議案無意見即達成共識，有意見則提出議案並有專家附議即進入討論程序，討論完畢投票表決，票數過半則該議案成立，不過半再繼續討論，共識程序如圖一。將「名義團體法」獲得共識的 EPAs 標題使用「修正式德菲法」(Modified Delphi Method, MDM) 進行共識程度投票，參與者基於 1 到 5 的李克特量表評估每個 EPAs 的“重要性”，其中 1 爲“不重要”，5 爲“非常重要，該議案四分位差小於 0.6 且五點量表大於等於 4 則保留該案件，共識程序如圖二。

結果

問卷調查結果

草案以公文方式寄至全國各核醫科後，共收集到 60 家核醫單位回覆 (答覆率=0.86 [60/70])。針對「同位素治療」提出 19 項修正案，14 項刪除案，4 項新增案，「核醫藥物與品保」提出 16 項修正案，8 項刪除案，12 項新增案。

表一　同位素治療 EPA、OPA 及觀察面向 (專家群草擬 / 共識前版本)

EPA	OPA	觀察面向
同位素治療	治療前準備	確認醫囑與病人辨識
		治療前簡易衛教說明
		備妥治療用品及設備
		環境鋪設
		輻射安全防護
	執行同位素治療	量測並記錄藥品劑量
		依醫囑完成同位素治療
		執行輻射安全偵測
		病人安全照護與突發狀況處理
		其他異常狀況判別及處置 (含團隊溝通)
	治療後處置	執行病人治療後衛教
		環境清潔與維護
		完成治療紀錄並歸檔
		造影及影像品管作業
		作業場所輻射防護監測

表二　核醫藥物與品保 EPA、OPA 及觀察面向 (專家群草擬 / 共識前版本)

EPA	OPA	觀察面向
核醫藥物與品保	使用前準備	目視設備是否正常
		目視所有指示燈功能是否正常
		測試電腦連線功能是否正常
		執行品保作業
	執行藥物偵測	背景值歸零
		設定偵測核種參數
		正確放置藥物
		正確偵測藥物活度
	使用後處置	設備使用紀錄
		藥物活度紀錄
		環境清潔
		汙染偵測

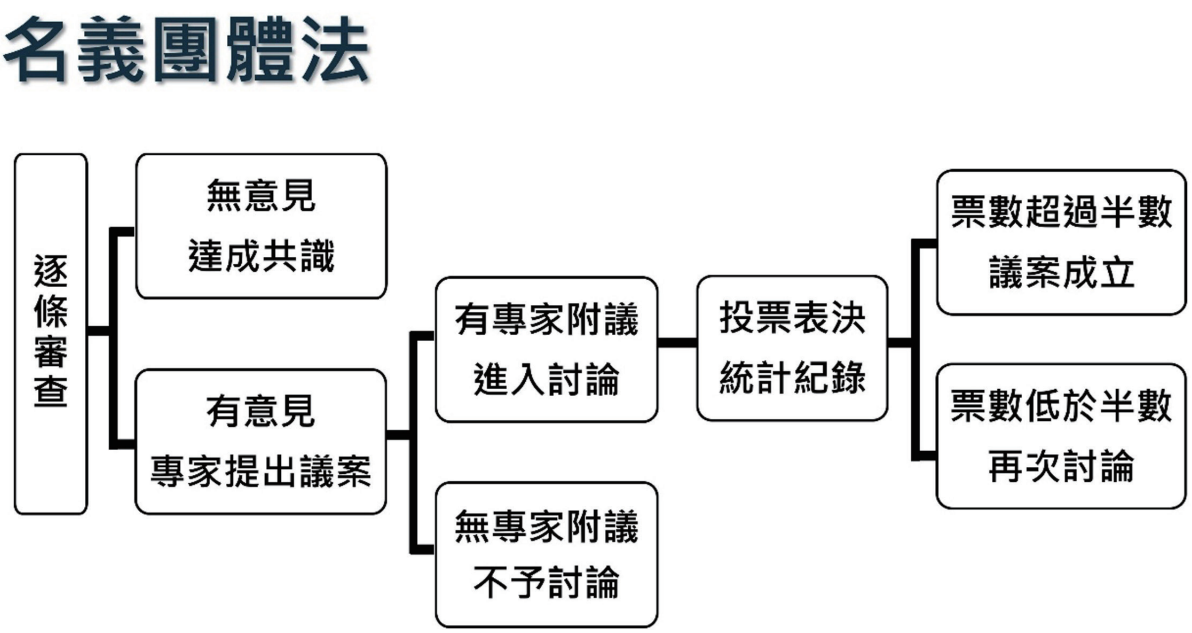

圖一　「名義團體法」共識程序

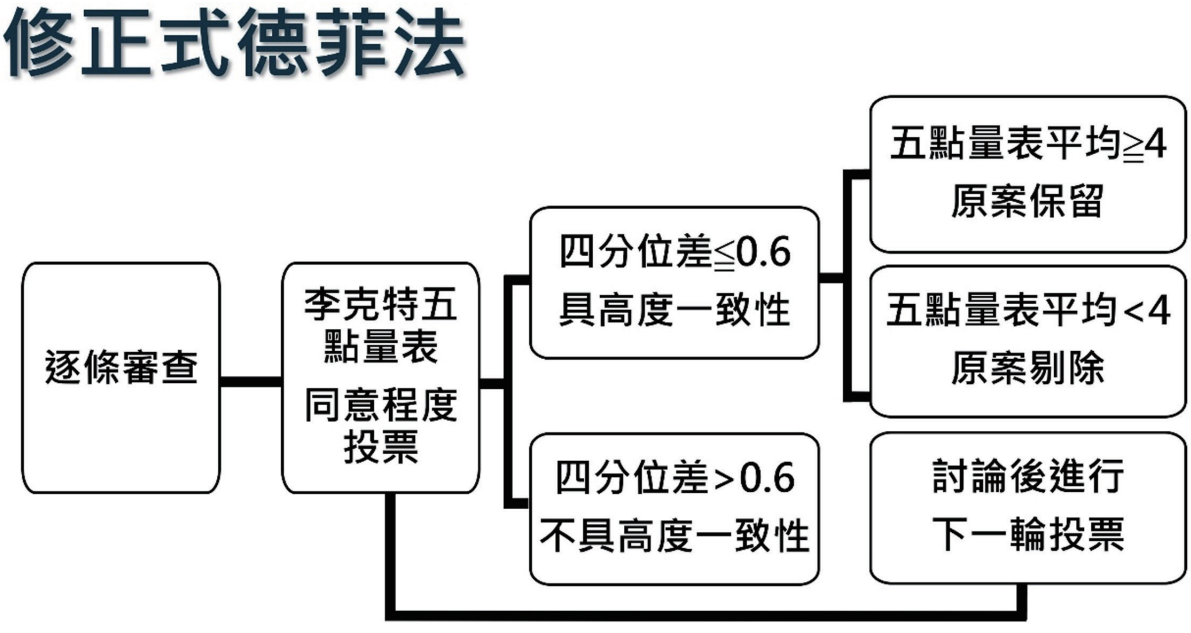

圖二　「修正式德菲法」共識程序

觀察面向討論及共識

使用「名義團體法」進行 EPAs 下各任務名稱觀察面向的討論，討論過程中部分案件以撤案方式處理，「同位素治療」一共撤除 9 項修正案，11 項刪除案，4 項新增案，「核醫藥物與品保」一共撤除 8 項修正案，2 項刪除案，11 項新增案，其餘案件進入討論及表決程序，一共進行 42 項次的團體表決，表決後 18 項次維持原名稱，9 項次修改觀察面向名稱，8 項次合併觀察面向，7 項新增案撤案；共識完成之「同位素治療」與「核醫藥物與品保」版本如表三、表四。將「名義團體法」獲得共識的 EPAs 標題以提案方式，使用「修正式德菲法」進行共識程度投票，33 項次提案進入表決程序，所有提案四分位差均小於 0.6，「同位素治療」EPAs 平均共識程度爲 4.89 分 (±0.10) (表三)，共識程度最低爲該項 EPAs 名稱同位素治療 (4.6 分)，共識程度最高爲造影及影像品管作業 (5 分)；「核醫藥物與品保」EPAs 平均共識程度爲 4.91 分 (±0.08) (表四)，共識程度最低爲背景值歸零與環境清潔與維護 (4.76 分)，共識程度最高爲輻射安全防護 (5 分)。

討論

相較於傳統教學法，CBME 擁有以下優勢，包括：以學生爲學習中心、強調實踐能力、持續評估與反饋、彈性調整學習時間…等，希望透過 CBME 的推動，希望能夠更全面地培養學生的專業知識和實踐能力，促進其綜合素質的全面發展，更好地應對現代醫療環境的挑戰。EPAs 便是其中一種讓 CBME 能夠從概念架構落實於教學訓練評估中的具體工具。

本次全聯會進行核醫領域 EPAs 建置，採用了「名義團體法」(NGT) 與「修正式德菲法」(MEM) 兩種常用的共識制定方法。名義團體法的優勢在於能快速激發眾多想法，並鼓勵多元意見的表達，非常適合用於初始階段的腦力激盪 [13]，爲後續的修正式德菲法提供豐富的素材。修正式德菲法則能有效減少群體壓力，讓專家們更客觀地評估每個 EPAs 項目。透過開放式討論，專家們能逐步縮小差異，最終達成高度共識。這種結合 NGT 與 MEM 的兩階段式方法，已成功應用於其他領域。例如，Zaeri 等人運用此法爲伊朗的健康職業教育博士學程制定 EPAs[14]；Pugh 等人將此法應用於加拿大內科住院醫師床邊手術技能的評估 [15]。NGT 與 MEM 的結合，能有效地協助核醫領域的專家們建立客觀、可靠且具有共識性的 EPAs 指標，爲核醫 CBME 的發展提供紮實的基礎。

表三　全國專家共識版本之同位素治療 EPA 及全國共識度

EPA	OPA	觀察面向	四分位差	平均值
同位素治療			0	4.61
	治療前準備		0	4.88
		確認醫囑與病人辨識	0	4.94
		治療前衛教說明	0	4.88
		備妥治療用品及設備	0.5	4.64
		環境輻射安全	0	4.94
		感染管制	0	4.94
	執行同位素治療		0	4.94
		量測並紀錄藥物劑量與時間	0	4.94
		依醫囑完成同位素治療	0	4.88
		執行輻射安全偵測	0	4.88
		病人安全照護與突發狀況處理	0	4.91
		異常事件之處置	0	4.97
	治療後處置		0	4.91
		執行病人治療後衛教	0	4.85
		環境清潔與維護	0	4.97
		完成治療紀錄並歸檔	0	4.94
		造影及影像品管作業	0	5
		作業場所輻射防護監測	0	4.91

表四 全國專家共識版本之核醫藥物及品保 EPA 及全國共識度

EPA	OPA	觀察面向	四分位差	平均值
核醫藥物及品保			0	4.94
	使用前準備		0	4.94
		確認設備功能	0	4.94
		執行品保作業	0	4.85
		感染管制	0	4.94
		輻射安全防護	0	5
	執行藥物活度偵測		0	4.94
		背景值歸零	0	4.76
		選定偵測核種參數	0	4.82
		放置藥物與偵測活度	0	4.85
	使用後處置		0	4.97
		紀錄存查	0	4.94
		環境清潔與維護	0	4.76
		作業場所輻射防護監測	0	4.97
		異常事件之處置	0	4.97
		紀錄存查	0	4.97

2020 年全聯會第一次召開全國共識會議，建置「正子電腦斷層造影檢查」與「單光子斷層造影檢查」EPAs 時，一共提出 41 項議案 (17 項修正案，7 項刪除案，17 項新新增案)。根據本次事前審查問卷回覆，共提出 73 項議案，由於國內各醫院核醫科作法不一致，包括執行人員非放射師 (由醫師、藥師或護理師執行)、部分單位無執行治療項目、使用的劑量校正儀廠牌不同，提供功能不一、多數單位無自行調製藥物，藥商提供單一劑量藥物…等，提出議案較前次多上許多，建置與共識難度更高，「同位素治療」刪除案件之部分原因爲非放射師執行該項目 (由醫師、藥師或護理師執行)，提出修改案則爲原因則爲名稱簡化或刪除、整併；「核醫藥物與品保」刪除案件之建議多爲項目合併，修改案原因多爲儀器設備不同，無法達到該項 EPAs 需求。經過「名義團體法」討論聚焦後最終定出 33 項提案進入「修正式德菲法」表決程序，所有提案四分位差均小於 0.6，且所有共識均通過，表示經過討論聚焦後所有專家對於所有議案有高度認同。

本次共識過程中，部分核醫專家認爲此兩份 EPAs 建置後恐有窒礙難行之處，一爲非放射師執行，一爲無相關項目，但以完整的放射師養成教育訓練整體觀來看，訓練計畫應包含所有項目，而訓練單位可針對受訓項目進行調整，最終所有核醫專家完成所有議案討論，經過數次討論過後逐漸聚焦並達成共識，完成全國專家共識版本之「同位素治療」及「核醫藥物與品保」EPAs。

表五 信賴等級及許可內容描述

信賴等級	許可內容
Level 1	僅隨側觀察。
Level 2a	教師監督，共同完成。
Level 2b	教師監督，適時協助。
Level 3a	間接監督，需逐項確認。
Level 3b	間接監督，重點確認。
Level 3c	間接監督，無須確認。
Level 4	可獨立執行。
Level 5	可執行教學。

共識版本之「同位素治療」及「核醫藥物與品保」EPAs 建置完成後，隨即建置即時評估 (ad hoc) 表單 (表單如附件，正式版本請上全聯會網站下載最新版本)，表單內含 EPAs 主題名稱、該 EPAs 情境說明、觀察學員後給予的信賴等級 (Entrustment-Supervision Level; ES level)，以及觀察操作後的質性回饋，其中信賴等級的訂定參考 Olle ten Cate 所制訂的監督等級，並採用了陳氏修正的ES量表，將信賴等級分爲等級 1 至等級 5 (表五)，其中等級 2 細分爲：2a、2b，等級 3 細分爲 3a、3b、3c，並明訂各信賴等級下許可內容說明，作爲臨床教師評核之參考依據 [7, 11, 12]。根據文獻指出，花蓮慈濟醫院急診部以急診醫學會公告 EPAs 版本爲藍本，調整或增加可觀察到的客觀事項進行評核，或某些重要概念在單一個案無法觀察到時，透過詢問方式，了解學員能力，執行成效良好 [16]。往後醫事放射職類各臨床教師進行

EPAs 評核時，可直接使用本研究共識之版本，直接進行各項信賴等級評分，並就觀察項目進行質性回饋，或是參考花蓮慈濟模式執行，應能獲得良好成效。

持續建置 EPAs 的同時，全聯會持續舉辦全國教育訓練，包括師資培育課程、推廣者工作坊、計畫主持人訓練、情境模擬臨床培訓…等，中華民國核醫學會醫技委員會亦在 2023 年進行全國推廣課程，分別於北北基區、北區、中區、南區開立教育訓練課程，透過種子教師逐步向下推廣 CBME。除積極新增多元評估工具之外，全聯會 2023 年與財團法人醫院評鑑暨醫療品質策進會「醫事專業人員能力進展資訊平台 (EMYWAY)」建置醫事放射職類 CBME 電子化學習歷程系統，未來希望透過 EMYWAY 整合所有訓練資訊。同時放射全聯會也自 2023 年 2 月 1 日開始進行爲期三年的 CBME 訓練計畫試辦醫院合作，希望透過試辦計畫，逐漸讓勝任能力爲導向的醫學教育在各醫院落地生根。

結論

本研究中，全聯會透過全國專家共識，完成「核醫藥物與品保」及「同位素治療」EPAs 建置，同時舉辦全國教育訓練課程及推廣教育，並藉由 CBME 試辦計畫，讓勝任能力爲導向的醫學教育落實於全國醫事放射職類核子醫學領域的醫學教育訓練與評估中。

致謝

本研究感謝中華民國醫事放射師公會全國聯合會 (全聯會) (TAMRT) ，感謝臺大醫院醫學教育專家楊志偉醫師，也感謝所有參與建置 EPAs 的核醫專家。

參考文獻

1. McGaghie, W., *Competency-based curriculum development in medical education: An introduction*. World Health Organization, 1978.
2. 蕭政廷 , 楊志偉 , and 周致丞 , *談如何在地落實 CBME: 以台灣急診醫學爲例* . 台灣醫學 , 2018. 22(1): p. 55-61.
3. 陳祖裕 , *可信賴專業活動的疑惑與理解* . The Changhua Journal of Medicine, 2017. 15(2): p. 104-113.
4. 譚健民 , 張維國 , and 楊銘欽 , *美國畢業後醫學教育評鑑委員會六大核心能力 -- 如何應用 [六大核心能力] 融入住院醫師教學訓練* . 2012.
5. 林文旆 , et al., *醫事放射師畢業後臨床訓練制度 (PGY)*. 2013.
6. Nasca, T.J., *The next step in the outcomes-based accreditation project*. ACGME Bull, 2008. 5: p. 2-4.
7. Ten Cate, O., *Entrustability of professional activities and competency-based training*. Medical education, 2005. 39(12): p. 1176-1177.
8. Boyce, P., C. Spratt, M. Davies, and P. McEvoy, *Using entrustable professional activities to guide curriculum development in psychiatry training*. BMC medical education, 2011. 11: p. 1-8.
9. Wagner, J.P., et al., *Use of entrustable professional activities in the assessment of surgical resident competency*. JAMA surgery, 2018. 153(4): p. 335-343.
10. 蔡孟軒 , 吳承誌 , 戴慶玲 , and 王郁青 , *藥學領域對於可信賴專業活動之認知 : 範域文獻回顧* . 臺灣臨床藥學雜誌 , 2021. 29(2): p. 75-82.
11. 黃國明 , et al., *醫事放射治療領域可信賴專業活動之建置與推廣 - 臺大醫院經驗分享* . 醫療品質雜誌 , 2020. 14(2): p. 52-57.
12. Tu, C.-Y., et al., *Development, implementation, and evaluation of entrustable professional activities (EPAs) for medical radiation technologists in Taiwan: a nationwide experience*. BMC Medical Education, 2024. 24(1): p. 95.
13. Harvey, N. and C.A. Holmes, *Nominal group technique: an effective method for obtaining group consensus*. International journal of nursing practice, 2012. 18(2): p. 188-194.
14. Zaeri, R. and R. Gandomkar, *Developing entrustable professional activities for doctoral graduates in health professions education: obtaining a national consensus in Iran*. BMC Medical Education, 2022. 22(1): p. 424.
15. Pugh, D., et al., *Using the entrustable professional activities framework in the assessment of procedural skills*. Journal of graduate medical education, 2017. 9(2): p. 209-214.
16. 胡勝川 , *里程碑和專業活動評核新攻略* . 臺灣醫界 , 2021. 64(1): p. 55-60.

Implementation of Entrustable Professional Activities (EPAs): Experiences at nuclear medicine field in Taiwan

Jui-Yin Kung[1,2,3], Kao-Yin Tu[1,4], Yu-Ching Hsu[1,5], Yi-Hsun Chen[1,6], Wan-Jo Chang[1,7], Chen-Jung Chang[3], Shih-Chuan Tsai[2,3#], Hui-Ping Chen[1,8*]

[1] *Taiwan Association of Medical Radiation Technologists*
[2] *Department of Nuclear Medicine, Taichung Veterans General Hospital, Taichung, Taiwan*
[3] *Department of Medical Imaging and Radiological Science, Central Taiwan University of Science and Technology, Taichung, Taiwan*
[4] *Department of Nuclear Medicine, Mackay Memorial Hospital, Taipei, Taiwan*
[5] *Department of Nuclear Medicine, Dalin Tzu Chi Hospital, Chiayi, Taiwan*
[6] *Department of Nuclear Medicine, Ditmanson Medical Foundation Chia-yi Christian Hospital, Chiayi, Taiwan*
[7] *Department of Nuclear Medicine, National Taiwan University Cancer Center, Taipei, Taiwan*
[8] *Department of Nuclear Medicine, Taitung Christian Hospital, Taitung, Taiwan*
[#] *S.C.T and H.P.C contributed equally to this work*

Abstract

In recent years, medical education has gradually shifted towards competency-based medical education (CBME). To ensure that the competency framework can be implemented in daily medical practice, Taiwan Association of Medical Radiation Technologists(TARMT) initiated the development of a nationwide consensus-based Entrustable Professional Activities (EPAs) form in 2020. In the same year, the nuclear medicine field completed EPAs forms for "Positron Emission Tomography (PET) Imaging" and "Single Photon Emission Computed Tomography (SPECT) Imaging." In this study, the TARMT planned to add two new EPAs, "Nuclear Medicine Drugs and Quality Assurance" and "Isotope Therapy." An expert panel was initially tasked with drafting the Observational Aspects for each Objective Practical Activity (OPA) within the EPAs. A nationwide survey was conducted in March 2023, and responses were received from 60 nuclear medicine units. On June 10, 2023, the TARMT held a national consensus meeting, inviting 43 medical education experts in the nuclear medicine field from across the country, including 18 representatives from (prospective) medical centers, 23 from regional hospitals, and 2 from local hospitals. The meeting began with an introduction to EPAs and consensus-building training by medical education experts, followed by the establishment of consensus and EPAs development. The Nominal Group Technique (NGT) was used to discuss and vote on the observational aspects of each task within the EPAs. A total of 42 group votes were conducted, resulting in 18 items with unchanged names, 9 with modified observational aspect names, 8 with merged observational aspects, and 7 new proposals withdrawn. Subsequently, the Modified Delphi Method (MDM) was used to vote on the degree of consensus, with consensus levels of 4.89 and 4.91 achieved, respectively. The development of the EPAs for "Nuclear Pharmacy and Quality Assurance" and "Radioisotope Therapy" was thus completed.

Keywords: competency-based medical education (CBME), Entrustable Professional Activities (EPAs), Nominal Group Technique (NGT), Modified Delphi Method (MDM)

J Nucl Med Tech 2024;21:47-60

Received 2024/12/20
Corresponding author: Shih-Chuan Tsai
Address: No. 1650, Sec. 4, Taiwan Blvd., Xitun Dist., Taichung City, Taiwan (R.O.C.)
Tel: 04-23592525#4800 ; Fax: 04-23741348
E-mail: sctsai@vghtc.gov.tw

Corresponding author：Hui-Ping Chen
Address: No. 350, Kaifeng St., Taitung City, Taitung County 950405 , Taiwan (R.O.C.)
Tel: 089-960888#8172 ; Fax: 089-341729
E-mail: a13026@tch.org.tw

附件

臺灣醫事放射職類可信賴專業活動評量表單

Entrustable Professional Activities (EPAs)

組別	□放射診斷□放射治療■核子醫學	日期	
地點		學員	
職級	□PGY1 □PGY2	教師	

一、主題

EPA3 同位素治療

■OPA1 治療前準備、□OPA2 執行同位素治療、□OPA3 治療後處置

二、情境說明

放射性碘治療案例觀察含分次治療及單次大劑量治療，治療流程依照各院規範及規模執行。

科內若放射師非主要執行業務項目，可與主要執行業務者聯合訓練。若院內執行其他放射性同位素核種治療業務，也可列入觀察項目。

三、信賴等級 (觀察學員後，您認為下次遇到類似情境此學員之勝任程度。)

評量項目 \ 信賴等級 LEVEL	不足/未評量	僅隨側觀察	教師監督，共同完成。	教師監督，適時協助。	間接監督，需逐項確認。	間接監督，重點確認。	間接監督，無須確認。	可獨立執行	可執行教學
	NA	**1**	**2a**	**2b**	**3a**	**3b**	**3c**	**4**	**5**
整體任務	■								
四、回饋參考內容									
(1) 確認醫囑與病人辨識									
(2) 治療前衛教說明									
(3) 備妥治療用品及設備									
(4) 環境輻射安全									
(5) 感染管制									

五、其他質性回饋

臺灣醫事放射職類可信賴專業活動評量表單

Entrustable Professional Activities (EPAs)

組別	□放射診斷□放射治療■核子醫學	日期	
地點		學員	
職級	□PGY1 □PGY2	教師	

一、主題

EPA3 同位素治療

□OPA1 治療前準備、■OPA2 執行同位素治療、□OPA3 治療後處置

二、情境說明

放射性碘治療案例觀察含分次治療及單次大劑量治療，治療流程依照各院規範及規模執行。科內若放射師非主要執行業務項目，可與主要執行業務者聯合訓練。若院內執行其他放射性同位素核種治療業務，也可列入觀察項目。

三、信賴等級 (觀察學員後，您認為下次遇到類似情境此學員之勝任程度。)

評量項目 \ 信賴等級 LEVEL	不足/未評量	僅隨側觀察	教師監督，共同完成。	教師監督，適時協助。	間接監督，需逐項確認。	間接監督，重點確認。	間接監督，無須確認。	可獨立執行	可執行教學
	NA	**1**	**2a**	**2b**	**3a**	**3b**	**3c**	**4**	**5**
整體任務	■								
四、回饋參考內容									
(1) 量測並記錄藥品時間									
(2) 依醫囑完成同位素治療									
(3) 執行輻射安全偵測									
(4) 病人安全照護與突發狀況處理									
(5) 異常事件之處置									

五、其他質性回饋

臺灣醫事放射職類可信賴專業活動評量表單

Entrustable Professional Activities (EPAs)

組別	□放射診斷□放射治療■核子醫學	日期	
地點		學員	
職級	□PGY1 □PGY2	教師	

一、主題

EPA3 同位素治療

□OPA1 治療前準備、□OPA2 執行同位素治療、■OPA3 治療後處置

二、情境說明

放射性碘治療案例觀察含分次治療及單次大劑量治療，治療流程依照各院規範及規模執行。

科內若放射師非主要執行業務項目，可與主要執行業務者聯合訓練。若院內執行其他放射性同位素核種治療業務，也可列入觀察項目。

三、信賴等級 (觀察學員後，您認為下次遇到類似情境此學員之勝任程度。)

評量項目 ＼ 信賴等級 LEVEL	不足/未評量	僅隨側觀察	教師監督，共同完成。	教師監督，適時協助。	間接監督，需逐項確認。	間接監督，重點確認。	間接監督，無須確認。	可獨立執行	可執行教學
	NA	**1**	**2a**	**2b**	**3a**	**3b**	**3c**	**4**	**5**
整體任務	■								
四、回饋參考內容									
(1) 執行病人治療後衛教									
(2) 環境清潔與維護									
(3) 完成治療紀錄並歸檔									
(4) 造影及影像品管作業									
(5) 作業場所輻射防護監測									

五、其他質性回饋

臺灣醫事放射職類可信賴專業活動評量表單

Entrustable Professional Activities (EPAs)

組別	□放射診斷□放射治療■核子醫學	日期	
地點		學員	
職級	□PGY1 □PGY2	教師	

一、主題

EPA4 核醫藥物與品保

■OPA1 使用前準備、□OPA2 執行藥物活度偵測、□OPA3 使用後處置

二、情境說明

輻射劑量活度計各院規範及規模執行。科內若放射師非主要執行業務項目，可與主要執行業務者聯合訓練。

三、信賴等級 (觀察學員後，您認為下次遇到類似情境此學員之勝任程度。)

評量項目 \ 信賴等級 LEVEL	不足/未評量	僅隨側觀察	教師監督，共同完成。	教師監督，適時協助。	間接監督，需逐項確認。	間接監督，重點確認。	間接監督，無須確認。	可獨立執行	可執行教學
	NA	**1**	**2a**	**2b**	**3a**	**3b**	**3c**	**4**	**5**
整體任務	■								
四、回饋參考內容									
(1) 確認設備功能									
(2) 執行品保作業									
(3) 感染管制									
(4) 輻射安全防護									

五、其他質性回饋

臺灣醫事放射職類可信賴專業活動評量表單

Entrustable Professional Activities (EPAs)

組別	□放射診斷□放射治療■核子醫學	日期	
地點		學員	
職級	□PGY1 □PGY2	教師	

一、主題

EPA4 核醫藥物與品保

□OPA1 使用前準備、■OPA2 執行藥物活度偵測、□OPA3 使用後處置

二、情境說明

輻射劑量活度計各院規範及規模執行。科內若放射師非主要執行業務項目，可與主要執行業務者聯合訓練。

三、信賴等級 (觀察學員後，您認為下次遇到類似情境此學員之勝任程度。)

評量項目 \ 信賴等級 LEVEL	不足/未評量	僅隨側觀察	教師監督，共同完成。	教師監督，適時協助。	間接監督，需逐項確認。	間接監督，重點確認。	間接監督，無須確認。	可獨立執行	可執行教學
	NA	**1**	**2a**	**2b**	**3a**	**3b**	**3c**	**4**	**5**
整體任務	■								

四、回饋參考內容

(1) 背景值歸零									
(2) 選定偵測核種參數									
(3) 放置藥物與偵測活度									

五、其他質性回饋

臺灣醫事放射職類可信賴專業活動評量表單

Entrustable Professional Activities (EPAs)

組別	□放射診斷□放射治療■核子醫學	日期	
地點		學員	
職級	□PGY1 □PGY2	教師	

一、主題

EPA4 核醫藥物與品保

□OPA1 使用前準備、□OPA2 執行藥物活度偵測、■OPA3 使用後處置

二、情境說明

輻射劑量活度計各院規範及規模執行。科內若放射師非主要執行業務項目，可與主要執行業務者聯合訓練。

三、信賴等級 (觀察學員後，您認為下次遇到類似情境此學員之勝任程度。)

評量項目 \ 信賴等級 LEVEL	不足/未評量	僅隨側觀察	教師監督，共同完成。	教師監督，適時協助。	間接監督，需逐項確認。	間接監督，重點確認。	間接監督，無須確認。	可獨立執行	可執行教學
	NA	**1**	**2a**	**2b**	**3a**	**3b**	**3c**	**4**	**5**
整體任務	■								
四、回饋參考內容									
(1) 紀錄存查									
(2) 環境清潔與維護									
(3) 作業場所輻射防護監測									
(4) 異常事件之處置									

五、其他質性回饋